Engineering Structures 318 (2024) 118759

Contents lists available at ScienceDirect

Engineering Structures

journal homepage: www.elsevier.com/locate/engstruct

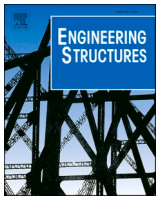

Time-domain fatigue reliability analysis for floating offshore wind turbine substructures using coupled nonlinear aero-hydro-servo-elastic simulations

Fengshen Zhu [a], Baran Yeter [a,b,*], Feargal Brennan [a], Maurizio Collu [a]

[a] Department of Naval Architecture, Ocean and Marine Engineering, University of Strathclyde, Glasgow, UK
[b] AAU Energy, Aalborg University, Niels Bohr 7, 6700 Esbjerg, Denmark

ARTICLE INFO

Keywords:
Offshore wind
Floating
Coupled AHSE
Fatigue
Fracture
Structural reliability
Monte Carlo simulation
Bootstrapping

ABSTRACT

The present study aims to develop a novel methodology for the fatigue reliability analysis and design for a floating offshore wind turbine substructure using its fully coupled nonlinear dynamic responses in the time domain. The developed methodology offers a computationally efficient yet robust assessment for designing fatigue-critical welded joints on floating substructures. The methodology starts with the sea state selection based on the fatigue damage contribution of all the sea states in the scatter diagram. To this end, the dynamic response is analysed by fully coupled aero-hydro-servo-elastic simulations using OpenFAST. The resulting short-term fatigue loading is then used to estimate the hotspot stress history using the analytical solution for global structural analysis and the empirical solution for the stress concentration factor. The long-term fatigue damage is calculated as the joint probability-weighted sum of the short-term fatigue damage using Palmgren-Miner's linear damage rule. Afterwards, the selected sea states are used to perform dynamic response simulations with multiple random seeds, ensuring no significant accuracy loss. To obtain the probabilistic fatigue life prediction, a novel time-domain fatigue reliability analysis algorithm is developed based on the bootstrapping method, which creates a pool of short-term fatigue responses with different random seeds and combines them within a Monte Carlo Simulation. Finally, the fatigue reliability analysis considering the S-N and damage-tolerant approaches for design is carried out.

1. Introduction

In pursuit of the UN's vision for tackling the energy trilemma – sustainable, affordable, and reliable energy for all, offshore wind has become a crucial sector within the renewable energy landscape. The offshore wind industry's success was predominantly fuelled by governments' incentives, eased financing, and cost reduction in manufacturing and construction, resulting in a low entry barrier for many private entities. However, the economic conjuncture changes as financial costs increase, and a future with lower government incentives is envisioned. Therefore, the offshore wind industry needs to make significant strides on the manufacturing and construction cost front whilst fully harnessing the offshore wind potential.

Floating offshore wind turbines play a crucial part in this challenge because they are uniquely positioned to tap into unexploited deep offshore sites with less turbulent wind potential, i.e. higher capacity factors. Furthermore, innovative solutions integrating floating substructures with green hydrogen production and storage units can address the intermittency pitfall of renewable energy, which is transformative for the renewable energy sector in terms of energy resilience [1,2].

The semisubmersible is the preferred substructure for floating offshore wind turbines (FOWT) owing to its inherent static stability by distributing buoyancy widely, less restrictive draft for port access, and streamlined installation and transportation process. Nevertheless, the high cost of manufacturing, including raw materials and labour, is an obstacle to overcome to achieve the desired levelised cost of energy. To this end, design optimisation that ensures structural integrity throughout service life with minimal cost is vital.

A point of concern for such structures is the welded-tubular joints connecting the central column to the side columns, as they are subjected to a high number of cycles due to both wind and wave-induced load cycles during service life. This brings forward the high-cycle fatigue as driving design consideration for hotspots around the welded joint with a potential to initiate cracks, as highlighted by DNV [3]. Moreover, a decentralised semisubmersible FOWT concept accommodating hydrogen production and storage on the top of side columns raises safety

* Corresponding author at: Department of Naval Architecture, Ocean and Marine Engineering, University of Strathclyde, Glasgow, UK.
E-mail address: baran.yeter@strath.ac.uk (B. Yeter).

https://doi.org/10.1016/j.engstruct.2024.118759
Received 6 March 2024; Received in revised form 10 July 2024; Accepted 6 August 2024
Available online 11 August 2024

Nomenclature

UN	United Nations
FOWT	Floating Offshore Wind Turbine
DNV	Det Norte Veritas
AHSE	Aero-Hydro-Servo-Elastic
MCS	Monte Carlo Simulation
S-N	Stress-Life
DTD	Damage-tolerant Design
TLP	Tension-Leg Platform
PRISMA	Preferred Reporting Items for Systematic Reviews and Meta-Analyses
ABS	American Bureau of Shipping
IEC	International Electrotechnical Commission
O&G	Oil and Gas
CFD	Computational Fluid Dynamics
PICO	Population, Investigation, Comparison, and Outcomes
IEA	International Energy Agency
NREL	National Renewable Energy Laboratory
DOF	Degree of Freedom
FD	Fatigue Damage
RFC	Rainflow Counting
SCF	Stress Concentration Factor
SIF	Stress Intensity Factor
FORM	First-order Reliability Method
SORM	Second-order Reliability Method
FCG	Fatigue Crack Growth
TwrBsMy	Bending Moment at the Tower Base
H_s	Significant Wave Height
T_p	Peak Period
V_s	Expected (Mean) Wind Speed
$\Delta\sigma_{HSS}$	Hotspot Stress range
$\Delta\sigma_{nominal}$	Nominal Stress range
β	Diameter Ratio
τ	Thickness Ratio
γ	Slenderness Ratio
$g(X)$	Limit State Function for Stochastic Variable Vector X
n_i	Number of Cycles Occurred at i^{th} Stress Range
N_f	Number of Cycles to Failure at i^{th} Stress Range
P_f	Probability of Failure
X_{SS}	Modelling Uncertainty Related to Sea State Selection
X_{SCF}	Modelling Uncertainty Related to SCF
X_{SIF}	Modelling Uncertainty Related to SIF
X_{GLA}	Modelling Uncertainty Related to Global Load and Stress Calculation
X_{FCG}	Modelling Uncertainty Related to Fatigue Crack Growth
ΔK	Stress Intensity Factor Range
ΔK_{eff}	Effective Stress Intensity Factor Range
a_0	Initial Crack Size
a_c	Critical Crack Size
a_0/c_0	Aspect Ratio
Δa_i	Crack Growth Rate
A	The Paris Law coefficient
C_p	The Wheeler retardation coefficient
α_i	Direction Cosine
s_i	Sobol Index

concerns and emphasises the importance of effective fatigue design for such mission-critical structural details.

To address the pressing issue explained above, this study contributes to the literature by developing a reliability-based fatigue design methodology for floating offshore wind turbine substructures. The developed methodology integrates actual metocean data and state-of-the-art nonlinear Aero-Hydro-Servo-Elastic (AHSE) simulations with well-established local stress calculation processed within a probabilistic assessment framework. The areas where the study goes beyond the common well-established practices are the sea state selection algorithm developed to reduce the number of AHSE simulations and the bootstrapping technique implemented into the Monte Carlo Simulation to perform efficiently the structural reliability analysis based on the time-domain responses. Thereby, the methodology offers a computationally efficient yet robust assessment for designing welded-tubular joints on a FOWT substructure accounting for uncertainties based on the stress-life (S-N) approach and fracture mechanics approach i.e., damage-tolerant design (DTD).

The significant contribution of the present study stems from the corrections it provides to the conventional fatigue reliability analysis that are more suitable for ship and offshore Oil & Gas structures, but not so ideal for FOWT substructures due to the fully coupled nonlinear dynamic structural response. The first correction is related to the sea state selection for which the common approach is to use the probability of occurrence to select a group sea state representing long-term fatigue loading. However, this very rough estimate on the representative sea states is quite flawed because even a low probability does not always necessarily mean a low fatigue damage contribution. For this reason, our fatigue reliability analysis methodology involves a sea state selection algorithm that is fatigue damage contribution-based rather than probability-based, for both the S-N and DTD approaches.

The second correction is about the fatigue reliability analysis for which the conventional approach used for ships or Oil & Gas platforms would be performing the analysis based on the expected hotspot stress range that represents the long-term stress range distribution considering a limited number of sea states with only one random seed for the dynamic response analysis (or even spectral-based neglecting nonlinearities). This conventional methodology involves a much bigger assumption with respect to load and stress exposure of the structure and it does not account for the variable amplitude loading as well as the effect of different random seeds, which is critical for the successful design of FOWT substructures. The main objective of the present study is to develop a methodology that corrects the shortcomings of the conventional method related to stress ranges in an efficient way by simulating the nonlinear dynamic structural response of FOWT using fewer sea states with a sufficient number of random seeds.

1.1. Systemic literature review protocol

A systematic literature review enables a structured approach to review existing literature on a specific topic of interest in a transparent and reproducible manner. It starts with formulating a clear and focused research question, followed by locating the studies from a complete database, selecting, and assessing the quality of the studies, and ending with the synthesis and critical discussion of results. Applying relevant keywords in four phases enables filtering out the most pertinent studies, nonetheless, ensuring all relevant literature is captured. In this study, the systematic literature review employs the PICO framework to formulate the research question and the PRISMA framework to screen and synthesise the relevant literature. Fig. 1 illustrates the protocol followed to perform the systematic literature review in detail.

A bibliometric analysis can support the screening process, presenting objectively the development of important research subfields and applications within the scope of the overarching research question. Fig. 2 presents changes in the research focus with respect to the fatigue design of offshore wind support structures in the last twenty years (2002–2023) based on the Web of Science (WoS) database. The results of the bibliometric analysis infer that there is a dramatic increase in the number of

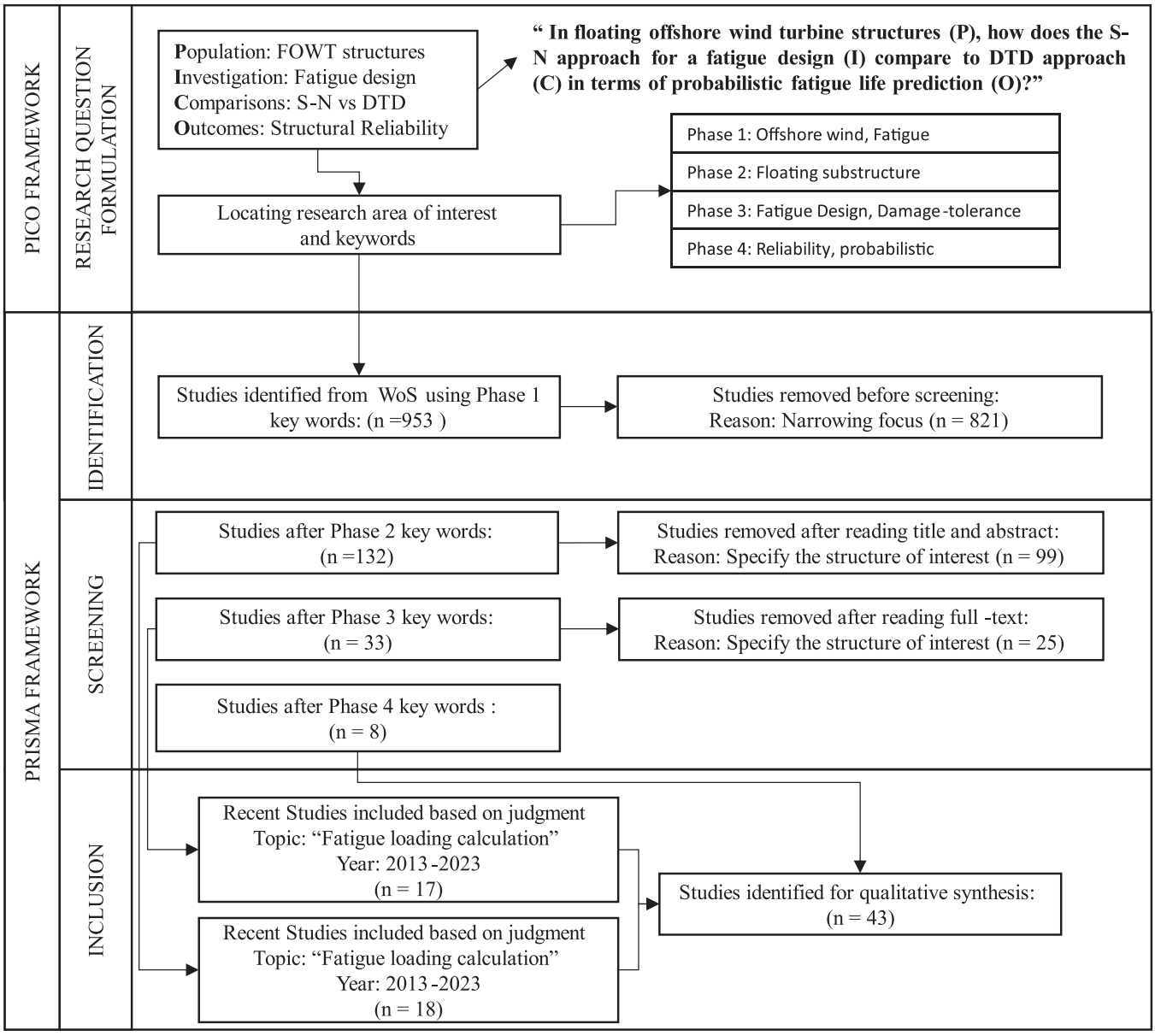

Fig. 1. Systematic literature review protocol.

studies related to the fatigue design of offshore wind turbine structures, which was initially driven by fixed-bottom structures, whereas the floating structures have gained attention, especially in the last few years. The chart on the top right shows the change in the number of studies related to fatigue design of floating substructures in two categories: a) fatigue loading analysis and b) fatigue damage analysis. There is a considerable amount of effort put into examining the nonlinear dynamic response of these floating substructures due to the complex coupling effect of environmental loading (wind, wave, current, etc.), mooring, control dynamics, and structural dynamics. Besides, addressing fatigue load by controlling wind turbine operation has recently gained importance. Last but not least, the design-oriented S-N approach is the more widely used approach in assessing the accumulated fatigue damage and fatigue life for FOWT substructures.

The present study finalises the systematic literature review by synthesising the findings from the selected studies in the form of a critical discussion. The critical discussion aims to evaluate the current state of the research field, "Reliability-based Fatigue Design Methodology for FOWTs" and identify gaps and emerging research directions in order to support the motivation of the present work.

1.2. *Literature review and critical discussion*

Offshore wind structures must be designed against cumulative fatigue damage failure caused by cyclic loading over their service life. To this end, the fatigue limit state can be defined by classification societies and industrial authorities such as DNV [3], ABS [4], and IEC [5], considering both fatigue loading and resistance aspects. These classification societies have traditionally recommended the stress-life (S-N) approach to deal with fatigue damage accumulation under the high-cycle loading regime, as the S-N approach is suitable for structures containing small defects under low load levels, i.e., elastic stress levels [6]. However, it is worth mentioning that most fatigue failures in offshore oil and gas structures stem from abnormal initial defects caused by welding processes and corrosion fatigue [7].

Alternatively, damage-tolerant design (DTD) is a fracture mechanics-based design approach dealing with the very nature of fatigue cracking under cyclic load. The DTD approach offers a better progressive damage

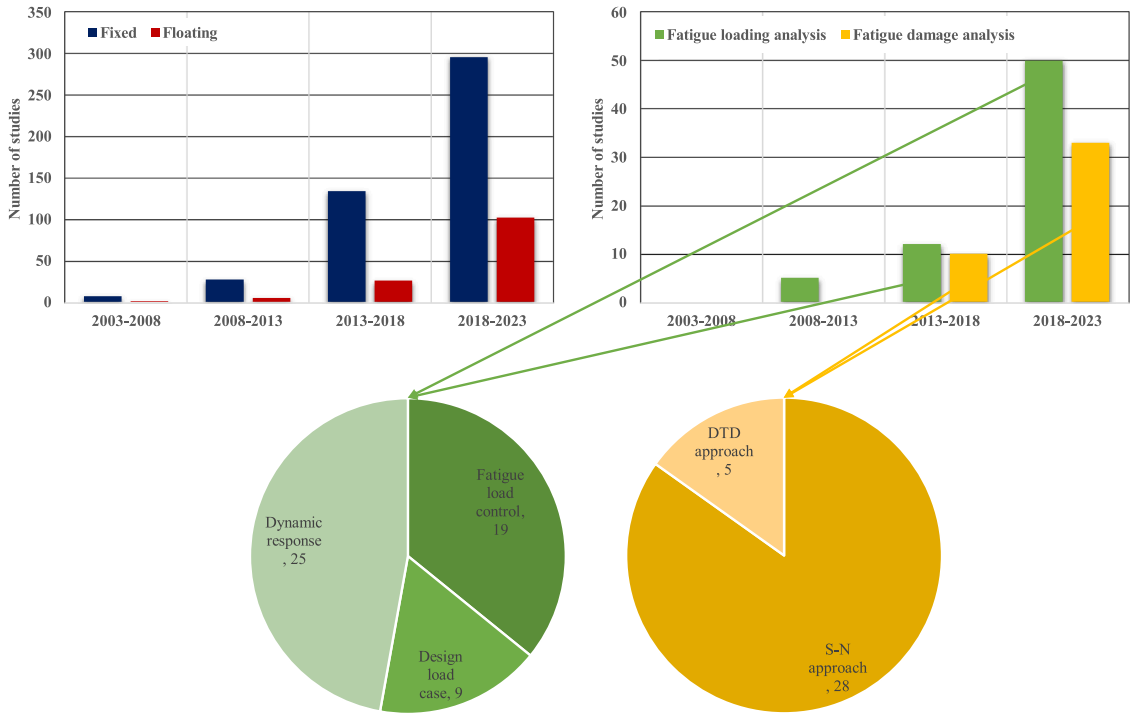

Fig. 2. Results of bibliometric analysis between 2003–2023.

modelling accounting for the effects such as corrosion [8,9], load sequence and retardation effects [10,11], and material properties characterisation [12]. Although a sophisticated damage model offers a more accurate fatigue life of the structure, the modelling uncertainty, in turn, fatigue life prediction increases. Thus, regardless of the opted design approach, S-N or DTD, a probabilistic structural integrity assessment accounting for uncertainties is vital for making better-informed decisions with respect to design [13,14], inspection planning [15] and end-of-life strategies [16].

For offshore wind structures, especially for floating ones, the coupling effect between wind and wave-induced loading is critical for the dynamic behaviour of the floating substructure [17], which directly influences the stress ranges and accumulated fatigue damage [18]. Although wind-induced loading is the dominating factor for fatigue consideration during operational conditions, as Xu et al. [19] argued, the contribution of wave-induced loading to the total fatigue damage can increase dramatically during sea states with high significant wave height. In this regard, Marino et al. [20] reported a substantial underestimation of the fatigue load due to the linear wave modelling during the parked condition.

In light of the discussion given above, the fully coupled time-domain load and structural response analysis using multi-physics numerical tools is the prescribed practice despite the computational effort as it captures the coupling effects arising from aerodynamic, hydrodynamic, elastic structural response, control systems, and boundary conditions [21]. Spectral-based and closed-form approaches offer practical alternatives to the time-domain solution, albeit with typically more conservative fatigue life estimates. Thus, these methods are useful for the initial screening purpose, pinpointing critical hotspots on complex steel structures with multiple welded-tubular joints [14].

The long-term fatigue damage assessment requires substantial computational effort due to the sheer number of numerical simulations performed to fully coupled dynamic responses in the time domain under several different environmental scenarios. In addition to this, these simulations need to be repeated numerous times for robustness in dynamic response and fatigue life calculations. To address this issue, Li and Zhang [22] suggested implementing a canonical vine (C-vine) copula model to represent the multivariate dependence of environmental conditions (wind speed and wave height) and an artificial neural network to predict short-term fatigue damage from the selected environmental parameters. Song et al. [23] also employed the C-vine copula method to develop a probabilistic model of environmental conditions with dependent parameters; however, the study's focus was primarily on the separation and segmentation of the metocean data prior to the C-vine copula method. This is particularly critical for the metocean data exhibiting non-stationarity behaviour due to seasonal variations and extreme weather effects (typhoons). The results of these two studies are significant, especially within the scope of probabilistic fatigue damage assessment. Although these studies are promising, it is worth noting that such an approach requires extensive and varied datasets to ensure accuracy in diverse environmental conditions.

Apart from the number of environmental conditions and statistical nature, there is also a sampling challenge due to the infinite potential load conditions. Using the bootstrap method, Song et al. [19] quantified the uncertainty associated with a finite number of load conditions considered in fatigue damage assessments. The study demonstrated that the uncertainty in the finite sampling of environmental conditions was significant enough to be included in the probabilistic fatigue damage assessment. By building upon the probabilistic model of environmental conditions [24] and the uncertainty analysis [23], Song et al. [25] later determined the representative load conditions to reduce the uncertainty by the Generalised F-discrepancy of the point set. Like the present study, integrating the Generalised F-discrepancy and copula method targeted the robustness of the time-domain fatigue damage assessment performed for FOWTs. Another study that acknowledged the uncertainties associated with environment load calculation and analysed their effect on fatigue reliability was reported by Hegseth et al. [26]. Hegseth et al. [26] showed that reliability-based fatigue design methodology could reduce the capital cost of the support structure by up to 11 %, which is considerable considering that the study merely focused on the random variables related to the environment load calculation (e.g. turbulence intensity, wind-wave misalignment, wind directional distribution, and a two-peak wave spectrum).

Wiley et al. [27] recently conducted a comprehensive sensitivity

analysis including 35 input parameters driving the structural design of the OC4-DeepCwind semisubmersible FOWT. The study concluded that turbulent wind velocity standard deviation was the parameter with the strongest global sensitivity as well as it contributes the most to the fatigue-proxy load. The study also observed the impact of random seeds on the sensitivity analysis eliminated after 20 random seeds; however, 20 random seeds for a fatigue damage assessment covering the whole scatter diagram most likely to require a very significant computational effort. Not for a floating OWT support structure but for a jacket one, Zwick and Muskulus [28] looked at the impact of multiple random seeds on the variability damage equivalent load (fatigue-proxy load) and showed that an uncertainty interval of $\pm$ 5 % is covered with 87.1 % and 94.9 % probability using 6 random seeds and 10 random seeds, respectively. Okpokparoro and Sriramula [29] suggested a coefficient of variation of nearly 20 % to the uncertainties incurred as a result of using 6 random seeds in the reliability analysis of FOWT dynamic cables.

These studies mentioned above demonstrate the importance of employing multiple random seeds in the fatigue damage assessment, nevertheless, the studies also indicate that there is an upper limit to which the benefit of using multiple random seeds diminishes. Such sensitivity analyses similar to the studies mentioned above require a significant amount of computational effort especially, this is arguably one of the reasons why the scope of the sensitivity analysis has not been extended to the fatigue reliability analysis. In addition to the above, the effect of environmental load uncertainty on fatigue reliability has been discussed in review studies such as [30,31]; however, these studies do not provide any quantitative results alongside such discussion.

There is a trade-off between the computational effort and accuracy for the time-domain fatigue damage assessment of a FOWT. In this regard, Müller and Cheng [32] adopted a quasi-random sampling based on Sobol sequences to reduce the number of Monte Carlo simulations needed to estimate the fatigue reliability of the FOWT. As suggested by Müller et al. [33], the Latin Hyper Cube random sampling within the Response Surface Method, or importance sampling and adaptive sampling within the MC simulation, and machine learning-based surrogate models [34] are other ways to reduce the computation effort for the fatigue reliability analysis.

In addition, the simulation length is an overlooked yet crucial factor influencing the computational cost-efficiency of fatigue damage assessment of FOWT. Haid et al. [35] assessed suitable simulation lengths for FOWTs and concluded that longer simulations did not lead to increased loads, indicating that the standard 10-minute simulation might be adequate for FOWTs. These results conflict with the well-established 3-hour simulation practice of the offshore O&G industry. An explanation could be that the contribution of the aerodynamic loads is expected to be higher than the hydrodynamic loads for the majority of the operating wind speed range; therefore, a 10-minute simulation depicting aerodynamic loads fully could suffice for FOWTs. More research is needed to confirm the results reported by Haid et al. [35], though.

Both the amplitude and frequency of environmental loadings influence the extent to which the wind- and wave-induced loads contribute to the total accumulated fatigue damage. At the rated wind speed, the thrust load, thus overturning bending moment, reaches its peak, resulting in a higher contribution from the wind-induced loading. However, wave-induced loadings are expected to be predominant as wave heights increase [36].

In terms of frequency, the second-order wave loads at lower frequencies can considerably affect the dynamic behaviour of FOWTs by inducing resonance at the eigenfrequencies of the floating substructure, as suggested by Zhao et al. [37]. Further, Zhao et al. [37] concluded that the effect of second-order wave loads would differ depending on the offshore wind turbine capacity as well as the floating substructure. The study performed by Cao et al. [38] also confirmed that at lower frequencies, second-order wave loads excite the pitch motion of the floating semisubmersible, leading to more serious fatigue damage. This is particularly important as second-order loads exhibited quadratic relationships with the significant wave height, which was claimed by Mei and Xiong [39], showing underestimated fatigue damage during extreme sea conditions when second-order hydrodynamic loads are ignored.

To improve the accuracy of available engineering models, Li and Bachynski-Polić [40] developed quadratic transfer functions based on the high-fidelity CFD model, whilst an uncertainty assessment of the impact of wave on the loading based on experimental data was presented by Robertson and Wang [41] to help validate numerical models with different levels of fidelity. Like wave-induced load modelling, wind-induced loading modelling can cause significant variation depending on the underlying assumptions of the modelling techniques. For instance, Doubrawa et al. [42] estimated that both Kaimal Spectrum Exponential Coherence and Mann turbulence models overpredicted fatigue loading in high wind speed scenarios by over 25 % and underpredicted it in low wind speed scenarios by nearly 20 %, whilst Putri et al. [43] observed near 30 % higher fatigue damage-equivalent load for the tower torsional moment for a very unstable atmosphere than neutral conditions, which points out the yaw mode of the semisubmersible FOWT.

Further to the physical and modelling uncertainties of the environmental loads of a FOWT, the short-term and long-term fatigue loading and damage are considerable variability due to phenomena, such as wake effects [44,45], operational conditions [46], wind-wave interactions [47] and directionality [48], slamming loadings [49], hydro-elastic behaviour of the large floating substructure [50,51], and fatigue loading control [52–56].

The success of accurate fatigue life predictions of FOWT is strongly contingent upon how well its dynamic behaviour is modelled. Unlike structural analysis under extreme events for the ultimate load limit state, fatigue analysis requires an extensive number of dynamic response analyses, covering the full scatter of sea states. According to the review by Otter et al. [57], the current state-of-the-art engineering models can offer low-fidelity to high-fidelity tools appropriate for innovative design where further optimisation is needed. To name a few examples, Matha et al. [58] analysed the coupled dynamic behaviour and performed the fatigue design of a concrete spar-type FOWT. Similar studies were conducted for a variety of different innovative substructures for FOWTs, such as tension leg spar-type [59], semisubmersible [60], Triple-Spar [61], and fully flexible TLP [62]. As stated by Otter et al. [57], there is an ongoing development using high-fidelity models to replace physical scale model testing when possible to accelerate the conceptual and preliminary design of FOWT.

By conducting a probabilistic fatigue damage assessment, i.e. fatigue reliability analysis, the uncertainties associated with the physical variability, modelling and measured data can be accounted for. However, so far, only a few studies have addressed fatigue analysis using probabilistic methods. Balli and Zheng [63] employed a pseudo-coupled approach to the fatigue assessment of VolturnUS-S semisubmersible FOWT, showing that long-term fatigue damage is quite sensitive to the changes in the main configuration of the substructure.

Although the fatigue analysis in the studies discussed above was based on the S-N design approach, the methodology introduced and underlying understanding regarding the load and numerical modelling uncertainties in these studies also applies to the DTD approach. In fact, Hegseth et al. [26] illustrated a rare example of fatigue reliability based on fracture mechanics for FOWTs, considering inspection planning adopted from the O&G industry's well-established structural integrity management procedure. In this regard, a note of caution can be the choice of initial crack size and the Paris Law coefficient, as these stochastic variables can cause significant variability in fatigue life [14,64].

The comprehensive literature review presented above revealed there are only a few studies so far, such as [23,24,26,32], addressing the probabilistic fatigue damage i.e. fatigue reliability of FOWT structures even though there is a significant consensus in the literature that a

FOWT's long-term dynamic structural response cannot be treated similarly to the conventional marine structures due to coupled Aero-hydro-servo-elastic dynamics. Therefore, the cost reduction that might be achieved by a probabilistic fatigue design is not completely explored yet, which puts the present study in a very strategically significant position.

The study presents the developed methodology in several phases, each of which tackles sub-objective and constituent tasks within a section. Section 2 gives an overall view of the methodology, the reference FOWT structure and model validation, which is followed by Section 3 delineating the relevant sea state selection to perform short-term fatigue loading analysis. Section 4 addresses the short-term structural response whose results are used to perform the fatigue damage assessment in Section 5. Subsequently, Section 6 explains the fatigue reliability analysis based on Monte Carlo Simulation (MCS) by explicitly representing the uncertainties through independent random variables. Section 6 also discusses two primary design philosophies: the stress-life (S-N) and damage-tolerant design (DTD) approaches. Lastly, Section 7 concludes the paper with final remarks and suggestions for future work.

2. Methodology

2.1. Methodology for fatigue reliability analysis based on time-domain simulations

The developed methodology is structured in multiple phases and commences with a data preprocessing of metocean, offshore site and structural configuration data. This phase is followed by the sea state selection process that chooses the sea states contributing the most to the accumulated fatigue damage, aiming to reduce the computational effort needed in the probabilistic long-term fatigue damage assessment. The examined full scatter is limited by the operating wind speed range (3 m/s – 25 m/s) for the fatigue limit state requisites [5].

In the long-term fatigue damage assessment covering a full scatter, 1-hour aero-hydro-servo-elastic (AHSE) simulations are carried out to obtain the bending moment at the tower base near the fatigue-critical tubular joint in question; subsequently, the hotspot stress-time history is derived by obtaining nominal stress using the analytical solution for the global structural analysis and combining it with the empirical stress concentration factor recommended by DNV [3].

Afterwards, the rainflow counting algorithm is used to count the stress ranges occurring over the course of service life for a given sea state, and the long-term fatigue damage is calculated by summing up the short-term fatigue damage associated with each sea state weighted by the probability of occurrence of the sea state throughout service life, which is given by the metocean data, as recommended by DNV [3].

The algorithm developed here to select sea states requires a threshold value between 0–100 per cent. For instance, a threshold value of 96 % means that the algorithm chooses the number of sea states that would guarantee a minimum of 96 % of the accumulated fatigue damage if all states were counted. Such a feature allows for a significant computational cost reduction with minimal accuracy loss, which can be accounted for later in the fatigue reliability assessment. Moreover, having fewer sea states increases the feasibility of performing the AHSE simulation with multiple random seeds, which has utmost significance in the probabilistic fatigue damage assessment using exact solutions such as crude Monte Carlo Simulation (MCS). Provided that there is not a statistically significant difference between the calculated fatigue damage using the considered simulation lengths, a number of random seeds higher than IEC [5] suggests can be used to ensure robustness in the bootstrapping method technique in MCS.

In the postprocessing phase, the bootstrapping technique is explored to produce an extensive number of combinations of short-term responses upon which the long-term fatigue damage can be calculated probabilistically. The study performs a fatigue reliability analysis using crude MCS with random sampling accounting for uncertainties such as material's fatigue strength, measurement, environmental condition, multi-physics modelling, global and local stress calculations, and damage modelling. Furthermore, two prominent design philosophies are compared: the stress-life (S-N) approach and the damage-tolerant design (DTD) approach. Fig. 3 illustrates the methodology introduced for reliability-based fatigue analysis and design for FOWTs in three phases: Preprocessing (data integration and analysis), Simulation (AHSE simulation and short-term fatigue damage assessment), and Postprocessing (structural reliability analysis based on MCS with bootstrapping).

2.2. Reference structure

The present study uses the "UMaine VolturnUS-S" semisubmersible platform as the reference floating substructure to support the 15 MW wind turbine developed by IEA [65]. Regarding the fatigue-critical structural detail to be designed, the welded-tubular joint at the tower base is chosen since the predominant wind-induced loading is distributed to the side columns through these tubular connections. Also, the failure of one of these tubular joints disrupts the whole operation of the offshore system at best and leads to catastrophic collapse at worst.

Fig. 4(a) illustrates the 15 MW "UMaine VolturnUS-S" FOWT and the dimensional and non-dimensional geometrical details of the structural detail are shown in Fig. 4(b). The non-dimensional geometrical details are particularly important for the empirical stress concentration factor equations to calculate local stress. Moreover, Table 1 presents the general system properties and the analysed structure's dimensions.

2.3. Site characteristics (Metocean data)

The offshore site planned for the deployment of the floating offshore wind turbine is situated within the Scottish sectoral marine plan, namely "NE8″, as shown in Fig. 5(a). The relevant metocean dataset is retrieved from the 5th generation European Centre for Medium-Range Weather Forecasts Reanalysis (ERA5), covering the period from January 1940 to the present [66]. The statistical descriptors related to the expected wind speed, significant wave height, and peak periods are derived using hourly metocean data from 2002 to 2021 (see Fig. 5(b)).

The statistical analysis indicates that the Weibull probability density function fits reasonably well to explain the expected wind speed, significant wave height, and peak period; however, the peak period can also be assumed to be explained by the Normal distribution. The statistical analysis can also suggest that the IEA15MW wind turbine with a rated power of 10.6 m/s complies very well with the offshore site characteristics, resulting in a high availability of offshore wind turbine operation.

The preprocessing of the metocean data categorises the expected wind speed with a bin width of 2 m/s between the operating wind speed IEA15MW wind turbine (3 m/s – 25 m/s) according to the recommendation of IEC 61400–3 [67]. For each wind speed bin, a two-dimensional scatter diagram is generated using the joint histogram between significant wave height and peak period with a bin width of 0.5 m and 1 s, respectively.

3. Fully coupled aero-hydro-servo-elastic simulation

3.1. Validation of the numerical model

The dynamic behaviour of a floating offshore wind turbine is nonlinear due to the complex interaction between the wind, wave, floating substructure dynamics and control systems. This nonlinear behaviour is best modelled and analysed using coupled aero-hydro-servo-elastic (AHSE) simulations performed in the time domain; thus, the current design practice prescribes time-domain simulations with complete turbine dynamics and control and simultaneous wind and wave loading [5]. For this reason, the present study uses OpenFAST, which is an open-source wind turbine simulation tool that was

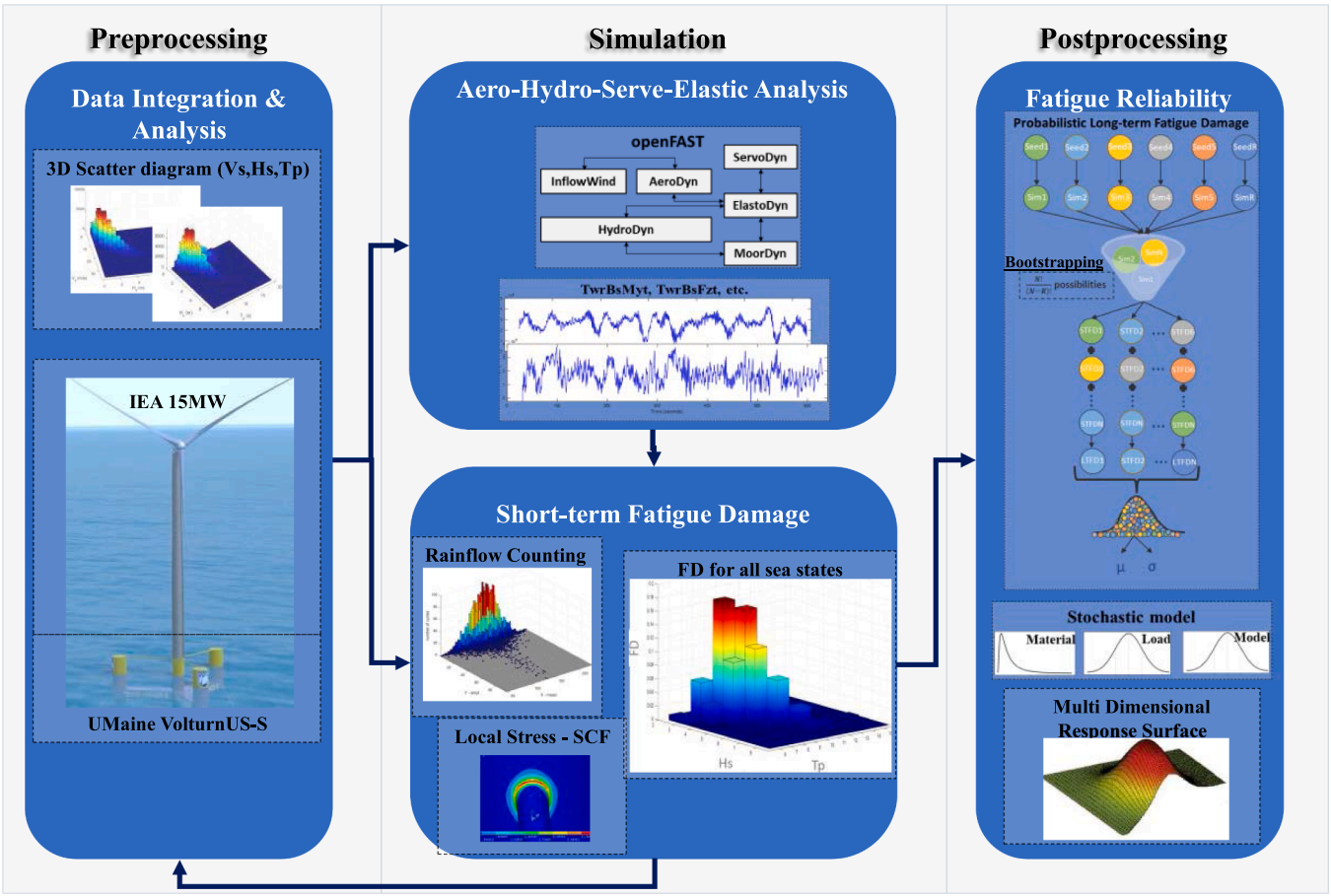

Fig. 3. Methodology developed to perform reliability-based fatigue analysis of FOWTs.

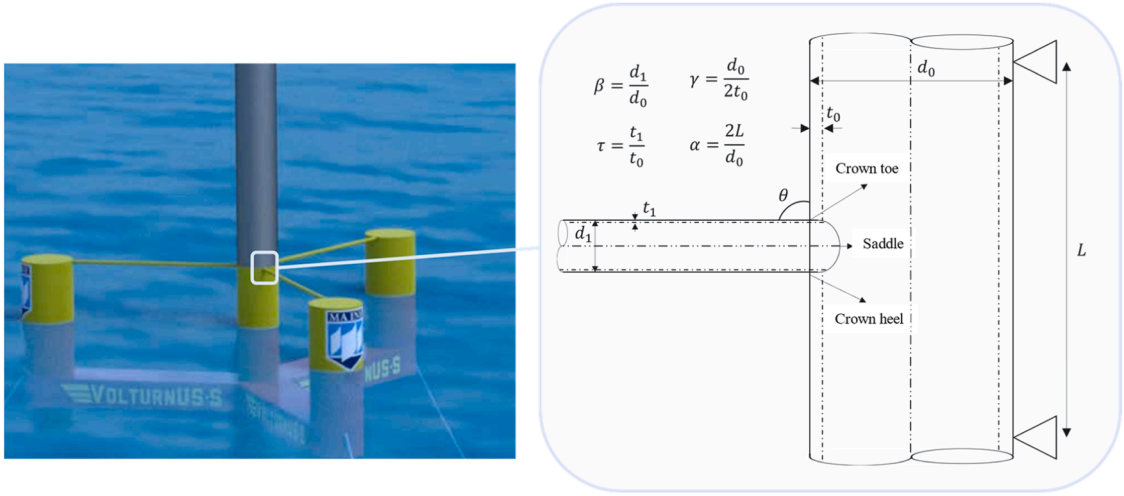

Fig. 4. Fatigue-critical welded-tubular joint of the FOWT in question (a) Location (b) Geometrical details.

developed by NREL [68,69].

Prior to performing the fully coupled AHSE simulations for the reference structure under the site-specific environmental conditions, it is essential to ensure that the numerical model is accurate. To this end, the numerical model is validated using natural frequencies in 6 DOF, such as surge, sway, heave, roll, pitch, and yaw, since these rigid body motions reveal valuable insights into the dynamic characteristics of the floating system. The results of the free-vibration analysis are compared with the results reported in IEA Wind TCP Task 37 [65], as given in Table 2.

Furthermore, Fig. 6 shows the rigid-body natural frequency of the floating substructure in 6 DOF in both time and frequency domains. The pitch motion is particularly noteworthy for the present study since it exacerbates the overturning bending moment occurring at the tower base when coinciding with the excitation coming from the wind loads. In

Table 1
General system properties of IEA 15 MW wind turbine supported by "UMaine VolturnUS-S" semisubmersible substructure.

Parameter	Units	Value
Wind turbine type	-	IEA−15 −240-RWT
Turbine Rating	MW	15
Hub Height	m	150
Rated (Power) Wind Speed	m/s	10.6
Freeboard (Tower base location)	m	15
Chord – Thickness (at tower base), t_0	mm	110 (originally 88.52)
Chord – Outer Diameter (at tower base), d_0	m	10
Brace – Thickness (at tower base), t_1	mm	22
Brace – Outer Diameter (at tower base), d_1	m	2
Effective length of the chord, L	m	50

addition, the natural frequency associated with heave lies within the wind spectrum's frequency range, which can influence the bending moment when coupled with the pitch motion.

3.2. Nonlinear dynamic behaviour analysis

A floating substructure is subjected to wind-induced loading transferred by the tower structure from the nacelle to the substructure, whilst the submerged part of the floating substructure is subjected to wave and current loads. Moreover, mooring connections provide translational restriction in all directions, which are connected to anchors, helping the FOWT to remain in place. The wind-induced loading, i.e. aerodynamic loading, stems from the wind forces acting on the blades, causing them to rotate. The resulting forces on the rotor plain can be divided into thrust and torque. Whilst thrust loads are transferred to the tower and floating substructure, the torque on the rotor determines the rotational speed and the mechanical energy converted from wind. Further, the wind speed varies stochastically around the stationary expected wind speed over a 10-minute time period due to turbulence, which can be modelled using wind spectra such as Kaimal.

Similar to the wind, the random nature of ocean waves can also be modelled using well-established wave spectra, such as Jonswap. In addition to the environmental loads, the period loads are related to the rotor's rotation (1 P) and blade passing (3 P). The elastic response of the tower and control dynamics also influence the loads acting on the floating offshore wind turbines. In order to take into account all the loads, AHSE simulations are performed in the time domain under the design load case prescribed for the fatigue limit state, which is DLC 1.2, as prescribed by IEC [5]. As explained in the previous section, the metocean data related to the "NE8″ offshore wind farm site are used to derive the expected wind speed, significant wave height and peak period for each sea state to perform a 1-hour AHSE simulation to obtain dynamic structural responses at the tower base. Based on the assumptions recommended for DLC 1.2, the normal turbulence model is used, no current loads are involved, and the wind and wave loads are considered unidirectional. The resulting overturning bending moment is then used to estimate the nominal stresses at the tower base. The present study only considered the overturning bending moment to estimate the nominal stresses since axial loads' contribution to the nominal stress is negligible.

The dynamic behaviour of the reference substructure is illustrated in the following figures in the time (up) and frequency domains (down) considering three distinct environmental conditions ranging from the wind speed around the rated power (10.6 m/s) to the wind speed near the cut-off limit (25 m/s). A transient period of 30 s is observed in the AHSE simulations; thus, the simulations are carried out for 630 s and the initial 30 s are cut off.

Fig. 7 shows the bending moment at the tower base (TwrBsMy) for a wind speed of 10 m/s (i.e., wind speed bin 9 m/s – 11 m/s), representing the conditions at which the wind turbine generates mostly its rated power. Fig. 8, on the other hand, represents an environmental condition where the thrust load is decreasing due to pitch control; however, the structure starts to be exposed to rough sea conditions. Fig. 9 illustrates how the substructure behaves when the expected wind speed is near the cut-off point (25 m/s) and wave heights are significantly higher than benign sea conditions.

Table 2
Rigid body natural frequencies.

Rigid body F_n	OpenFAST 3.5.0 simulation (Hz)	IEA Wind TCP Task 37 (Hz)
Surge	0.007	0.007
Pitch	0.033	0.036
Sway	0.007	0.007
Roll	0.033	0.036
Heave	0.047	0.049
Yaw	0.010	0.011

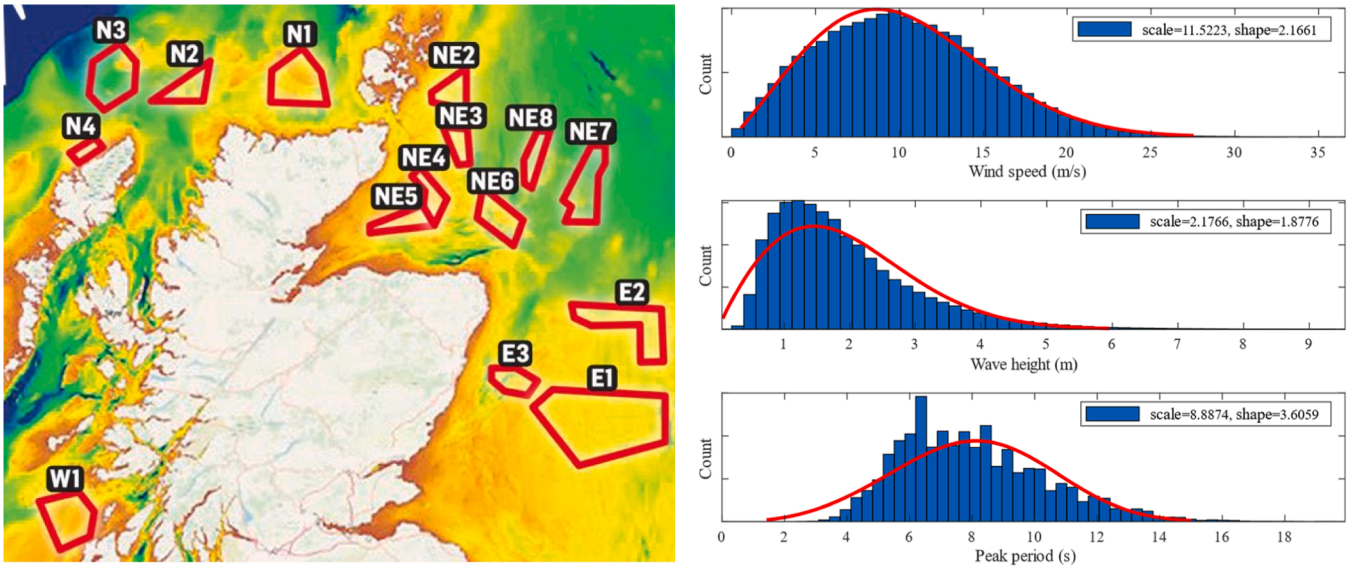

(a) (b)

Fig. 5. Offshore site (a) Scottish sectoral marine plan – NE8 (b) Statistical analysis of the metocean data.

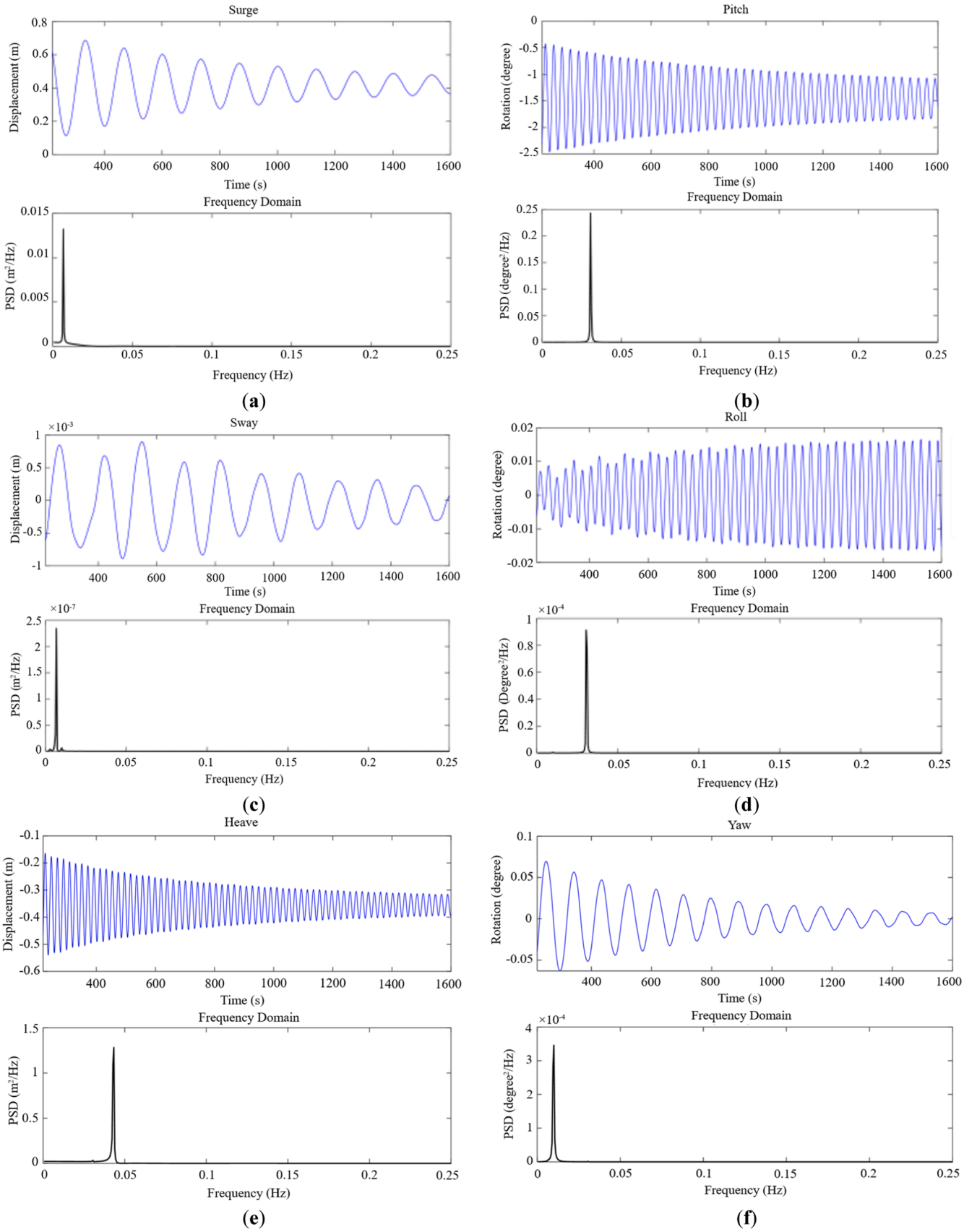

Fig. 6. Rigid body natural frequencies (a) Surge (b) Pitch (c) Sway (d) Roll (e) Heave (f) Yaw.

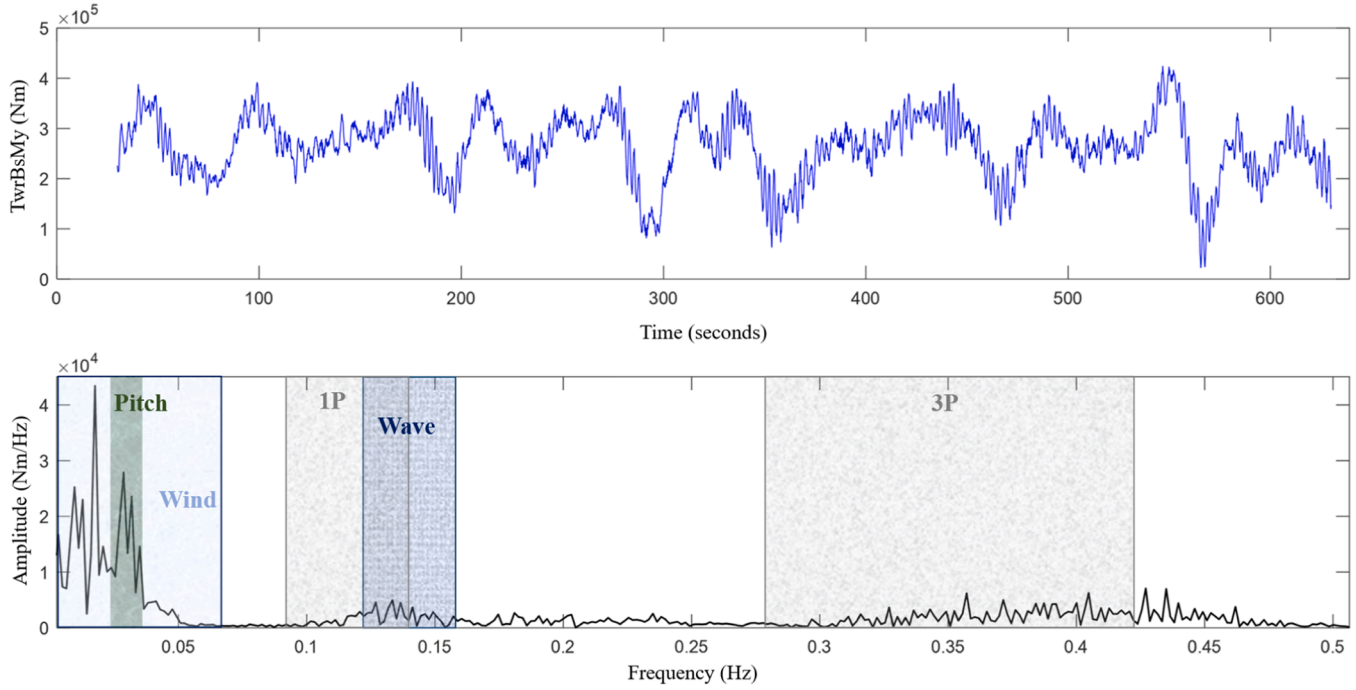

Fig. 7. $V_s = 10$ m/s, $H_s = 1.5$ m, $T_p = 6$ s.

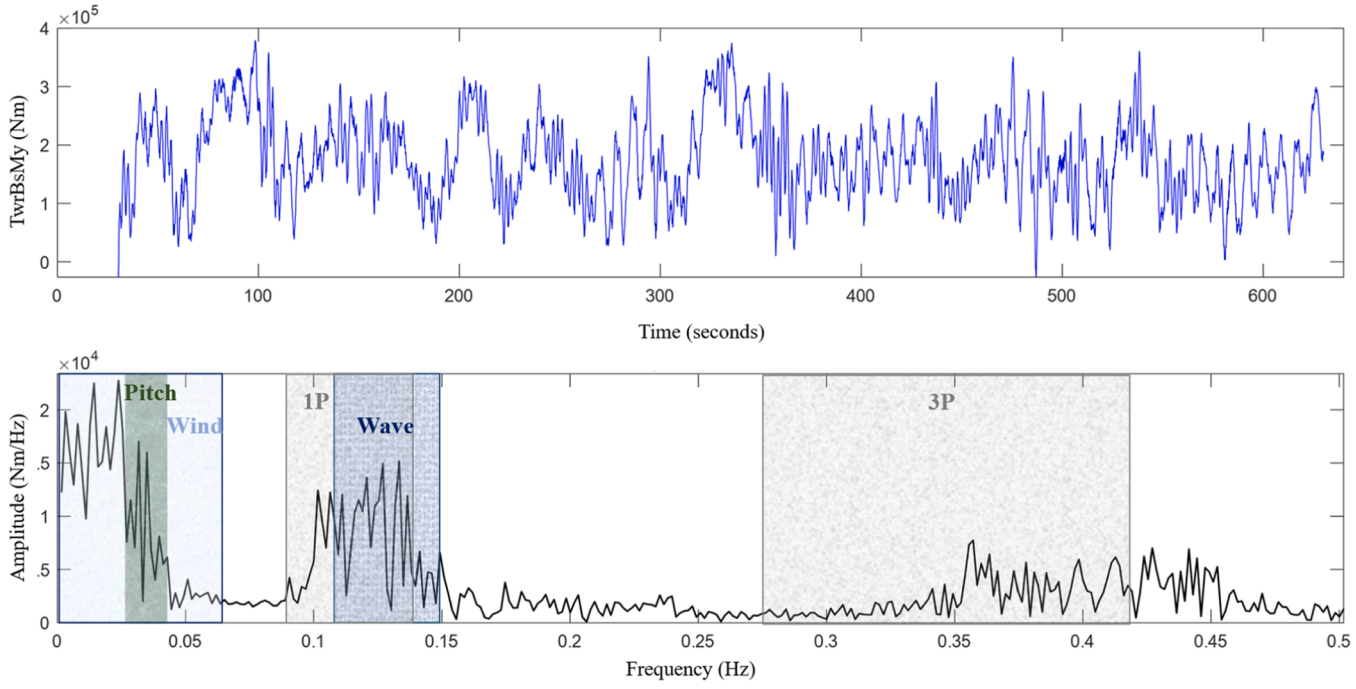

Fig. 8. $V_s = 16$ m/s, $H_s = 3$ m, $T_p = 8$ s.

In Fig. 7, the dynamic response in the frequency domain shows that the wind-induced loading is the predominant source of load, and the pitch response is pronounced as it is excited by wind loads as well. Fig. 8 illustrates that towards a higher wind speed and significant wave height, the dynamic response gets a comparable contribution from both wind and wave-induced loadings. Moreover, a higher peak period makes the dynamic response coincide more with the rotor frequency. Lastly, it is clear that the wave-induced loadings are the predominant source of load towards the end of the operating wind speed range (see Fig. 9). It is worth noting that that a transient period of 30 s is extended to 100 s for the simulations conducted within the fatigue damage assessment; the whole simulation is for 700 s where 100 s are cut off to ensure the structural dynamics are well-captured.

The results of the dynamic response analysis by AHSE simulations indicate that the contribution from the wind and wave loads varies depending not only on the magnitude of the load but also on the wind turbine's control strategy. To better illustrate that, a parametric study is designed under three scenarios: 1) stochastic wind and wave loads are coupled, 2) only stochastic wind loads are present, and 3) stochastic wave loads are coupled with a stable (static) wind load condition (no

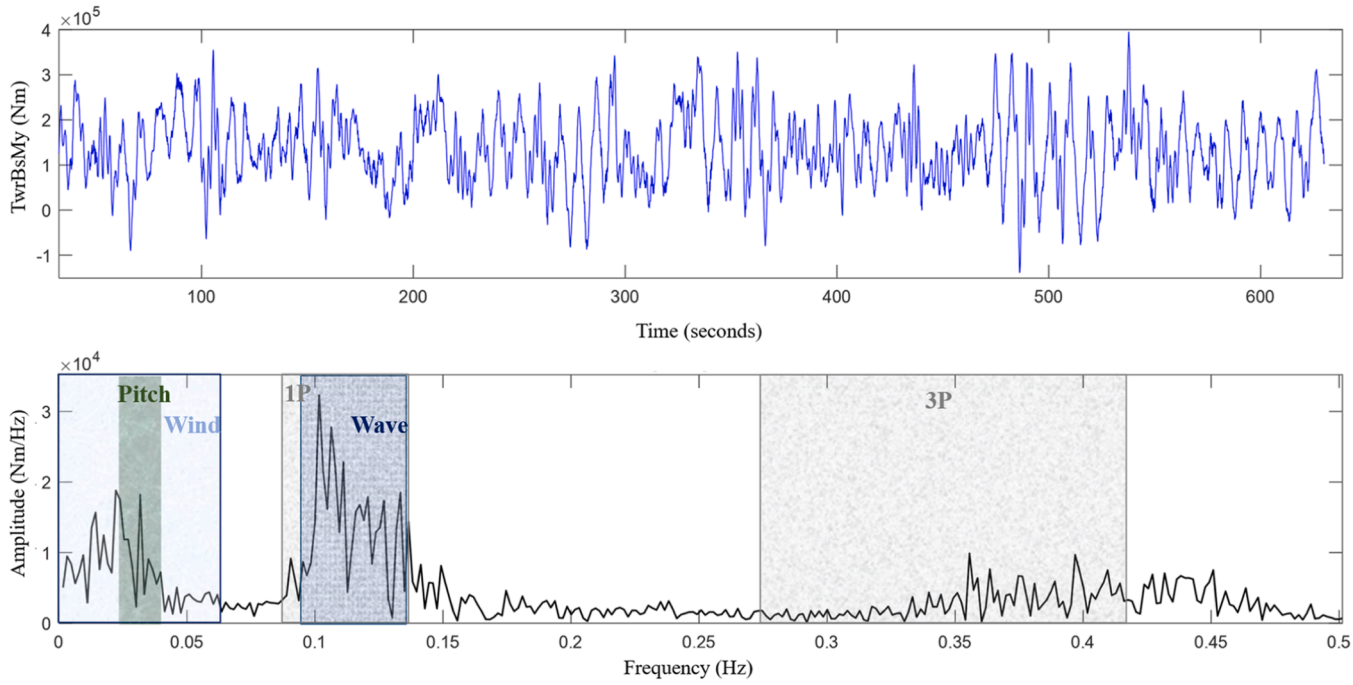

Fig. 9. $V_s = 22$ m/s, $H_s = 4.5$ m, $T_p = 9$ s.

turbulence).

Fig. 10 demonstrates how much the wind and wave loads contribute to the normalised short-term fatigue damage (FD) for the most probable sea state associated with each wind speed bin. Evidently, the turbulent wind load is the primary source of fatigue damage up to the wind speed of 14 m/s. However, from this point on, the benign sea conditions become harsher; thus, there is more contribution coming from the stochastic wave loads. Another reason for such a change is that pitch control changes the angle of attack, reducing the thrust loads. It is also worth mentioning that there is a need for further investigation with a more random realisation of wind and wave loads to statistically confirm the outcomes of this parametric study.

4. Algorithm for a cost-efficient sea state selection process

4.1. Sea state selection algorithm

An algorithm has been developed to assess the short-term fatigue damage of welded-tubular joints and identify the sea states contributing most significantly to long-term fatigue damage. The process begins with creating a database using hourly marine meteorological data, including information on wind, wave, and sea surface temperatures obtained from the Scottish Sectoral Marine Plan – NE8. Wind speed (V_s), significant wave height (H_s), and peak wave period (T_p) are evenly partitioned into intervals, represented by the mean values of their upper and lower limits. Subsequently, the probability of each sea state is determined by counting the occurrences of each state and dividing this count by the total number of sea states.

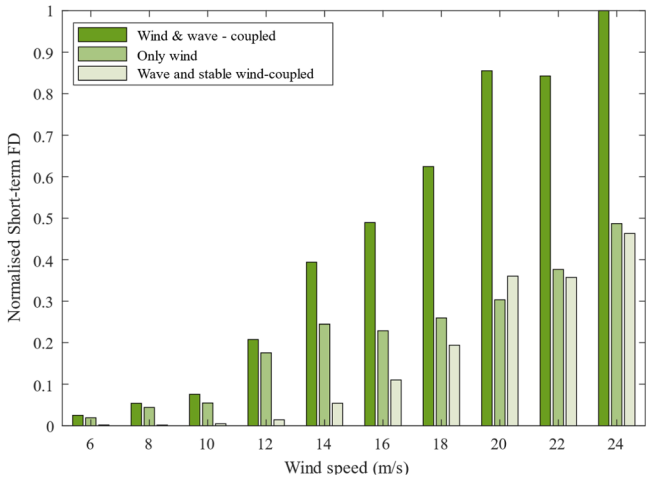

Fig. 10. Contribution of the wind and wave loads to the fatigue damage.

Following the metocean data preprocessing, the dynamic response of the tower base under various sea states in the time domain is obtained through the automated execution of OpenFAST. Once the primary structural configuration is defined, the hotspot stress-time history at the critical tubular joint susceptible to fatigue damage is estimated using the S-N approach utilising the rainflow counting (RFC) technique and factoring in the probability of each sea state allows for the computation of short-term fatigue damage. Accumulating the short-term fatigue damage from each sea state facilitates the calculation of long-term fatigue damage. The fatigue damage assessment based on the S-N approach using the hotspot stress time histories is a well-established design procedure and documented in DNV [3] and ABS [4].

Ultimately, the probability-weighted short-term fatigue damages are normalised based on the total fatigue damage, listed, and sorted in descending order. Then, depending on the user entry for the threshold value, the sea states contributing to the total fatigue damage the most are selected. By setting a threshold value that not only ensures the accuracy of long-term fatigue analysis but also minimises the number of simulations, sea states meeting the criteria can be accurately identified and outputted, leading to an optimal analysis process. This process is illustrated in Fig. 11, and the following section presents the details regarding fatigue damage assessment performed based on the S-N approach.

4.1.1. S-N approach for fatigue damage assessment

The fatigue limit state is paramount for non-redundant structures because hotspots (locations with stress risers) on the welded connections of FOWT structures can initiate small cracks under a sufficient number

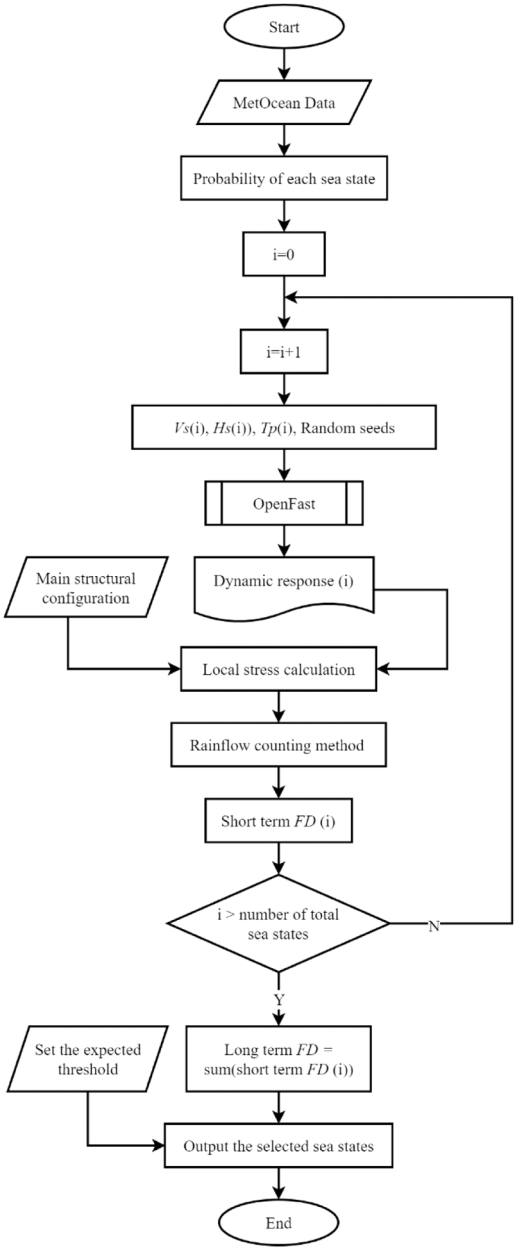

Fig. 11. Algorithm developed for sea state selection.

of cycles; as a result, these small cracks can eventually grow into a through-thickness rapidly leading to a fast fracture of the non-redundant member. Three overarching factors govern the fatigue damage and life prediction: 1) Local stress calculation, 2) Fatigue strength characterisation (varying with loading type, environment, and structural detail), and 3) Expected number of repeated stress cycles over the service life.

The hotspot stress approach has been widely employed within the S-N and DTD approaches to deal with the fatigue design of ship and offshore structures. The hotspot stress approach suggests weighting the nominal stress with a stress concentration factor (SCF), which can be obtained from empirical formulations based on experiments. Finite element analysis (FEA) can also be performed to obtain SCF; however, there are basic assumptions regarding thickness, finite element sub-model, structural configuration, mesh density, and extrapolation points [70], which leads to significant variability in fatigue life estimation as pointed out by Saini et al. [71]. The hotspot stresses σ_{HSS} used within the S-N approach are derived as follows [3,4]:

$$\sigma_{nominal} = \frac{M_y}{I_{yy}} y = \frac{M_y}{\frac{\pi}{32}\left({d_0}^4 - (d_0 - 2t_0)^4\right)} \frac{d_0}{2} \tag{1}$$

and

$$\sigma_{HSS} = \sigma_{nominal} SCF \tag{2}$$

where

$$SCF = 1.45\beta\tau^{0.85}\gamma^{(1-0.68\beta)}\sin\theta^{0.7} \tag{3}$$

where M_y, y, and I_{yy} are overturning bending moment, distance from the natural axis and the moment of inertia in the opposing direction of the bending moment. Also, σ_{HSS}, $\sigma_{nominal}$ and SCF are the hotspot stress, nominal stress and stress concentration factor for the crown position of the welded-tubular joint under in-plane bending loading. Further, SCF is estimated using an empirical formula derived from non-dimensional geometrical parameters related to the welded-tubular joint, assuming that the non-geometrical structural dimensions lie within the validity range (the thickness of the brace component is assumed). Also, note that σ_{HSS} is the stress amplitude at the hotspot; thus, the corresponding stress range $\Delta\sigma_{HSS}$ is calculated as 2 x σ_{HSS}.

Within the scope of the S-N approach, a set of international uniaxial S-N curves are used to characterise the fatigue strength of the material and connection [3,4]. The S-N approach involves finding the number of cycles n_i that occurred at critical areas of the structure at a given hotspot stress range $\Delta\sigma_{HSSi}$ and comparing them with the number of cycles to fail N_f given by the S-N curves, which are defined by the material characteristic, the detail of structure and the used stress method [72]. In light of the methodology described above, the fatigue limit state function described by the variable vector $\boldsymbol{X}$ can be written based on the Palmgren-Miner [73] rule:

$$g_{FLS}(\boldsymbol{X}) : D_{total}(\boldsymbol{X}) < 1 \tag{4}$$

where

$$D_{total} = \sum_{i}^{all} D_i p_i \tag{5}$$

where D_i is the short-term fatigue damage and p_i is the joint probability of the sea state (V_s, H_s, T_p) defining occurring during service life T_d, it is calculated as the ratio between the number of cycles occurred at the n and N_f as follows:

$$D_i = \sum_{i}^{all} \frac{n_i}{N_{f,i}} \tag{6}$$

where

$$\log N_{f,i} = \log\tilde{a} - m\log\left(\Delta\sigma_{HSS,i}\left(\frac{t}{t_{ref}}\right)^k\right) \tag{7}$$

where m is the negative inverse slope of the S-N curve, and $\log\tilde{a}$ denotes the intercept logN-axis, and it is proportional to the number of cycles the material can withstand before failure. The following expression describes analytically how the n_i is estimated using $\Delta\sigma_{HSS,i}$ in T_d seconds, and it can be expressed as:

$$n_i = f_i T_d \int_0^{\infty} p(\Delta\sigma_{HSS,i}) d\Delta\sigma_{HSS} \tag{8}$$

where f_i is the frequency at which $\Delta\sigma_{HSS,i}$ occurs. In the present study, n_i is calculated by employing the rainflow counting algorithm [74] using the hotspot stress response in the time domain for each sea state. The characteristic values of the parameters involved in the fatigue damage assessment are given in Table 3.

Based on the fatigue damage assessment methodology described above, the contribution from 834 sea states, full scatter diagram, are calculated and weighted with the corresponding probability of occurrence to estimate the long-term fatigue damage. The contribution from the sea states associated with different wind speeds to the long-term (total accumulated) fatigue damage (FD) is illustrated in Fig. 12. Fig. 12 reveals that for wind speeds (V_s) of 14 m/s, 16 m/s, and 18 m/s, there is a higher number of sea states with significant contributions to the long-term FD than those for 10 m/s and below, as well as 20 m/s and above. This result can be explained by the fact that the overturning bending moment is influenced by both wind and wave loads.

For the sea states involving the wind speed (10.6 m/s) at which the wind turbine is producing its rated power, the thrust load acting on the tower top is the primary source of overturning bending moment, which is also reflected in the hotspot stress ranges. Even though for higher wind speeds, blades are pitched to reduce the total wind forces acting on the blades, resulting in the thrust load reduction, higher significant waves dramatically increase the overturning moment at the tower base. Thus, it is reasonable to expect greater short-term fatigue damages from the sea states involving higher wind speeds and significant wave heights. However, when combined with the probability of occurrence, the sea states with higher contributions to long-term fatigue damage are found to be the ones related to the wind speed bin 14 m/s and 16 m/s. In this regard, Fig. 13 demonstrates the distribution of the probability of occurrence, normalised short-term fatigue damage and the short-term sea states' contribution to the accumulated fatigue damage together.

It is of utmost importance to reduce the computational effort needed for the fatigue damage assessment, which requires cumbersome simulations for many sea states. The algorithm presented in this section essentially addresses this issue by introducing a threshold parameter as input by the user; thus, the number of sea states contributing to the long-term fatigue damage assessment is reduced. The threshold parameter, ranging from 0 to 100, serves as the loss of accuracy that the user is willing to accept in exchange for fewer sea states for which the fully dynamic simulations should be carried out, which is also extremely critical for the probabilistic assessment needing random realisation of these simulations. To this end, a parametric study is conducted to analyse and quantify the change in accuracy.

Fig. 14 shows the parametric study results considering two simulation lengths, 600 s and 3600 s. It is possible to make the case that out of 834 sea states (full scatter), approximately one-eighth fraction of the full scatter (102 sea states) contributes the majority (80 %) of the long-term fatigue damage.

The argument above is valid for the simulation length of 600 as well as 3600 s. Therefore, it is possible to reduce the computational effort significantly by taking into account the sea states contributing the most, assuming that the loss of accuracy can be compensated in the probabilistic assessment by a random variable with a mean value of 1 plus the loss of accuracy in percentage. For instance, the present study proceeds with the 296 sea states covering 96 % of the full scatter, leaving the loss of accuracy to be 4 %; then, the fatigue damage assessment is modelled by a random variable with a mean value of 1.04.

It is worth noting that the number of sea states to be included to achieve a unit percentage of (long-term fatigue damage) accuracy increased dramatically around 95 % ($\pm$ 1 %). So long as the accuracy loss due to using fewer sea states is added to the final fatigue damage estimate, the fatigue reliability results are not expected to be affected by this loss because the variability within the total fatigue damage estimates is very low and consistent across different accuracy levels.

Furthermore, the parametric study can be extended to examine the difference between different simulation lengths in terms of the resulting long-term fatigue damage. It is a common practice to perform a coupled dynamic response simulation for an hour to capture all frequency ranges from wind and wave spectra. However, the difference arising from a relatively shorter simulation might not be substantial for long-term fatigue loading. Fig. 15 shows how the long-term fatigue damage changes with respect to different simulation lengths. The results indicate that there is not a strong relation between the simulation length and conservatism of the fatigue damage estimate; therefore, it is reasonable to assume that carrying out the fatigue damage assessment using the 600-second-long simulations would not affect the integrity of the analysis.

Moreover, due to shorter simulations in addition to the fewer number of sea states, the cost-efficiency of the probabilistic fatigue damage is improved immensely without compromising the accuracy. Thus, the coupled dynamic analysis for each considered sea state involved a minimum of 10 random seeds for the uncertainty of environmental loads captured sufficiently. These coupled dynamic analyses with 10 random seeds represent the short-term fatigue loadings, which are to be combined randomly using a bootstrapping technique to derive the long-term fatigue loading.

Table 3
Characteristic values.

Parameter	Description	Value
T_d	Service life	25 years
m_1	Negative inverse slope for $\Delta\sigma_{HSS} > \Delta\sigma_{Limit}$	3
m_2	Negative inverse slope for $\Delta\sigma_{HSS} \leq \Delta\sigma_{Limit}$	5
$\log\tilde{a}_1$	Intercept of logN axis for $\Delta\sigma_{HSS} > \Delta\sigma_{Limit}$	12.164
$\log\tilde{a}_2$	Intercept of logN axis for $\Delta\sigma_{HSS} \leq \Delta\sigma_{Limit}$	15.606
$\Delta\sigma_{Limit}$	Fatigue limit at $\sim 10^7$	52.63 MPa
k	Thickness exponent	0.25
t_{ref}	Reference thickness	32 mm

5. Probabilistic fatigue damage assessment

Monte Carlo Simulation (MCS) is a stochastic technique for numerical integration using random variables. MCS can approximate the probability of failure by employing random sampling of the variables within a limit state function, representing uncertainties for structural failure problems. These uncertainties can be aleatory (material properties, environmental loads) and epistemic (modelling, statistical). When performed with a vast number of random samples, the technique converges the most accurate structural reliability estimate [75].

The biggest advantage of the MCS technique is that it enables probabilistic structural assessment, where analytical solutions, such as time-domain fatigue damage assessment, are not available. Moreover, MCS can accommodate many uncertainties with non-normal distributions, making the technique a versatile tool. Although the MCS technique can be computationally demanding, high-performance computing significantly increases its practicality. For low probabilities of failure, the first-order reliability method (FORM) and second-order reliability method (SORM) can be advantageous in terms of computational efficiency; however, the intermediary process, such as the derivation of the long-term stress range distribution and uncertainty associated with the modelling makes the use of FORM and SORM less accurate alternatives to the Monte Carlo Simulation [76].

The structural reliability is calculated based on the very idea that a limit state function divides n-dimensional variable space into two regions, "safe" and "unsafe". Thus, the probability of failure of a structural component concerning a single failure mode can be formulated as follows:

$$P_f = P[g(\mathbf{X}) \leq 0] = \int_{g(X)\leq 0} f_X(\mathbf{X})dx \tag{9}$$

where $g(\mathbf{X}) = (X_1, X_2, \ldots, X_n)$ denotes the limit state function, $f_X(\mathbf{X})$ denotes the joint probability density function of the essential variables, and P_f stands for the probability of failure. Assuming that a dataset of short-term fatigue loadings $S = \{S_{11}, S_{12}, S_{13}, \ldots, S_{ij}\}$ can be defined for i number of random seeds and j number of sea state, a long-term stress history $B_k = \{S_{l1}, S_{l2}, S_{l3}, \ldots, S_{lj}\}$can be generated by bootstrapping with

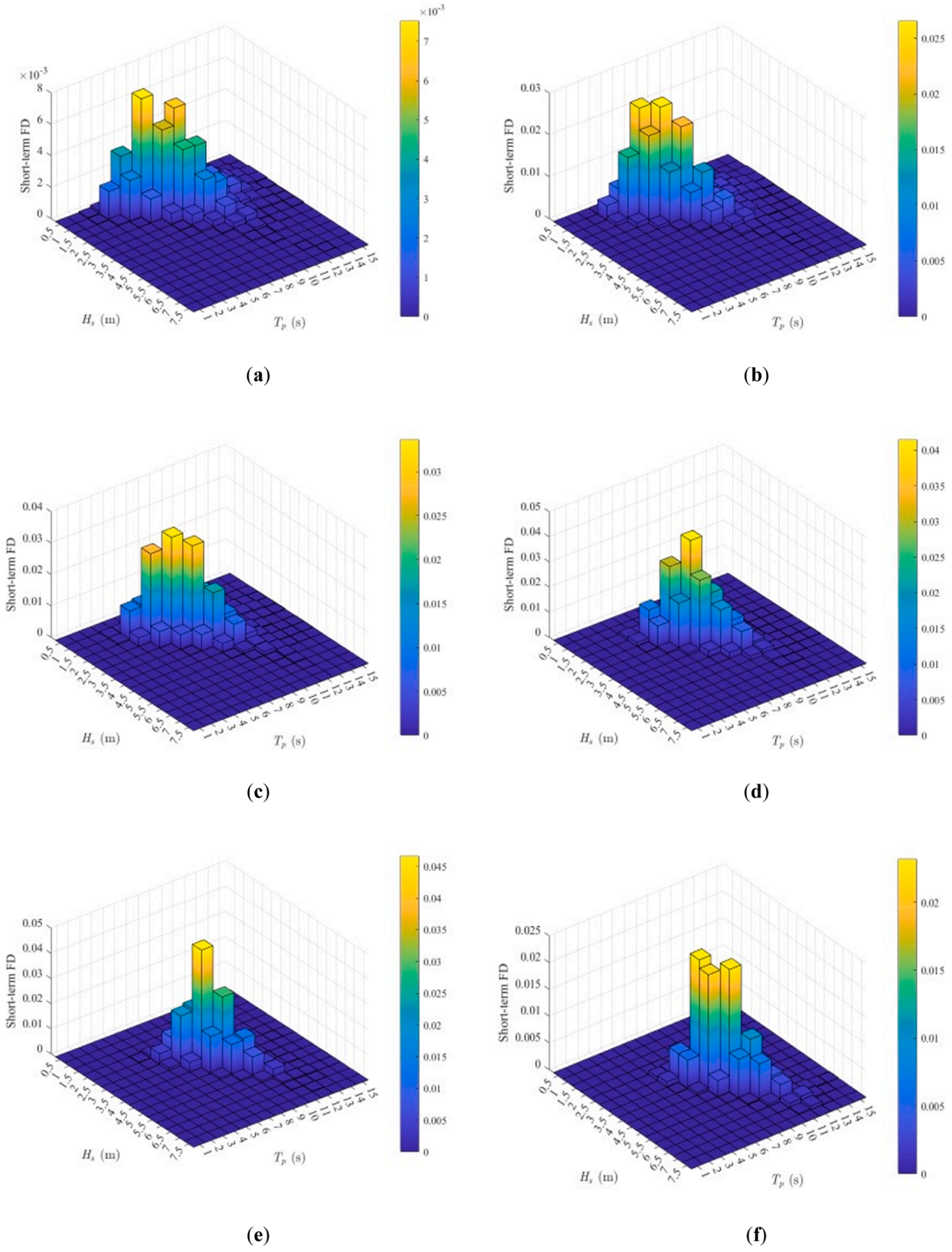

Fig. 12. Probability-weighted short-term fatigue damage (FD) (a) $V_s = 10$ m/s (b) $V_s = 12$ m/s (c) $V_s = 14$ m/s (d) $V_s = 16$ m/s (e) $V_s = 18$ m/s (f) $V_s = 20$ m/s.

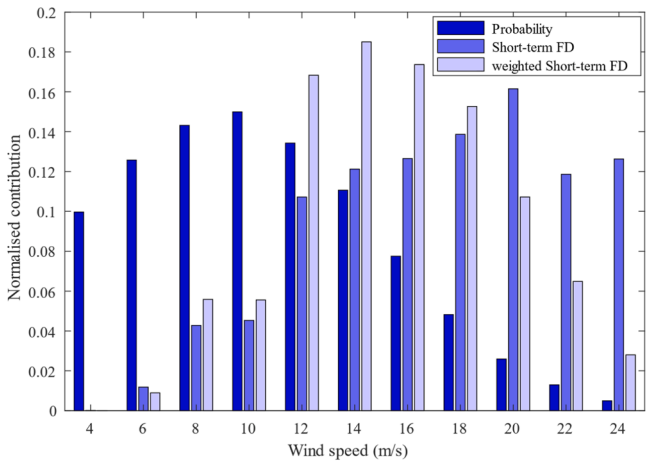

Fig. 13. Distribution of probabilities, short-term FD, and weighted short-term FD over the range of operating wind speed.

replacement where $S_{lj} \in S$ and $l \sim$ Uniform(1,i) expresses the random index by which the fatigue loading for sea state j is drawn from the dataset. By doing so, the long-term stress history B_k can be randomly generated for N times, and the probability of failure and structural reliability index can be calculated by the Monte Carlo Simulation (MCS) method as:

$$P_f = \frac{1}{N}\sum_{1}^{N} I(X_i) \tag{10}$$

where

$$I(X) = \begin{cases} 1, & \text{forg}(X) \le 0 \\ 0, & \text{forg}(X) > 0 \end{cases} \tag{11}$$

and

$$\beta = -\Phi^{-1}(P_f) \tag{12}$$

where Φ^{-1} is the inverse standard normal probability density function, and β is the reliability index.

For comparison purposes, the conventional approach to the fatigue reliability analysis using the expected hotspot stress range distribution within the analytical solution of the fatigue damage accumulation is explored. The first-order reliability method is used to solve the structural reliability problem by approximating the standard normal distributed failure domain by a half-space fit to the true failure domain at the most expected failure point β. The probability preserving transformation $x = T(u)$ where u is an independent standard normal vector, which transforms the probability integral into [77]:

$$P_f = \int_{g(X)\le 0} f_x(x)dx = \int_{g(T(u))\le 0} \varphi_U(u)du \tag{13}$$

where $\varphi_U(u)$ is the n-dimensional standard normal density with independent components. The analytical solution of the accumulated fatigue damage is provided by DNV [3] as:

$$D = \frac{n_0}{\tilde{a}} q^m \Gamma(1 + m/h) \tag{14}$$

where $q^m\Gamma()$ accounts for the expected value of the long-term $\Delta\sigma_{HSS}$ and n_0 is the number of cycles occurred during the service life, assumed to be 10^8.

The stochastic variables involved in the probabilistic long-term fatigue damage assessment are presented in Table 4. It is worth noting that the loss of accuracy due to reducing the number of sea states involved in the calculation is compensated by introducing a stochastic variable X_{SS}. The other stochastic variables are related to the material's fatigue strength log$\tilde{a}$, global load and stress analysis X_{GLA}, stress concentration factor X_{SCF}, and fatigue damage accumulation D [78–80].

The crude MSC is performed to estimate the accumulated fatigue damage at 5, 10, 15, 20, and 25 years to demonstrate how structural reliability changes over time. To this end, a process that decreases the number of trials in MCS is implemented; for instance, the fatigue reliability analysis considering the first five years is simulated with 50000 trials. For the fatigue reliability analysis considering 10, 15, 20, and 25 years, the number of trials is reduced to 40000, 30000, 20000, and 10000.

As shown in Fig. 16, in all cases, a sufficient number of trails are simulated to yield a stable mean value and standard deviation of the long-term fatigue damage, which results in the necessary confidence in calculating the reliability index, i.e. probability of failure. Furthermore, Fig. 17 shows how the histograms of the long-term fatigue damage vary over the course of service life based on the stochastic variables introduced. These histograms are fit to a Weibull distribution whose shape factors remain the same, indicating the relative dispersion does not

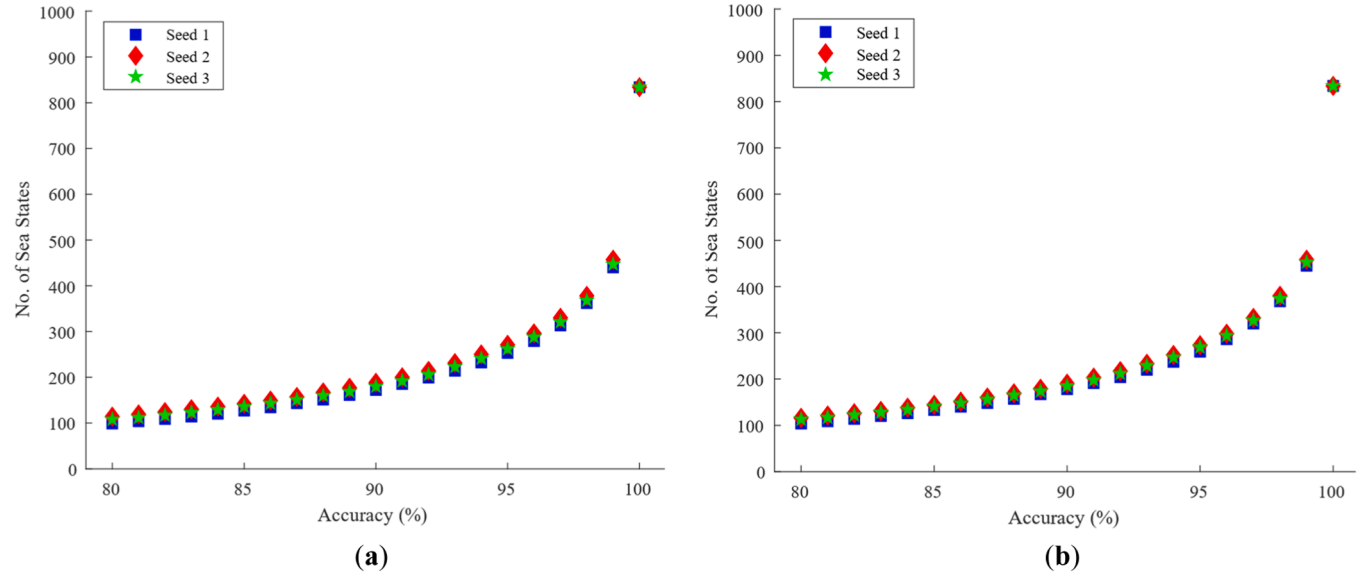

Fig. 14. Change in the accuracy with respect to the number of sea states (a) 600 s (b) 3600 s.

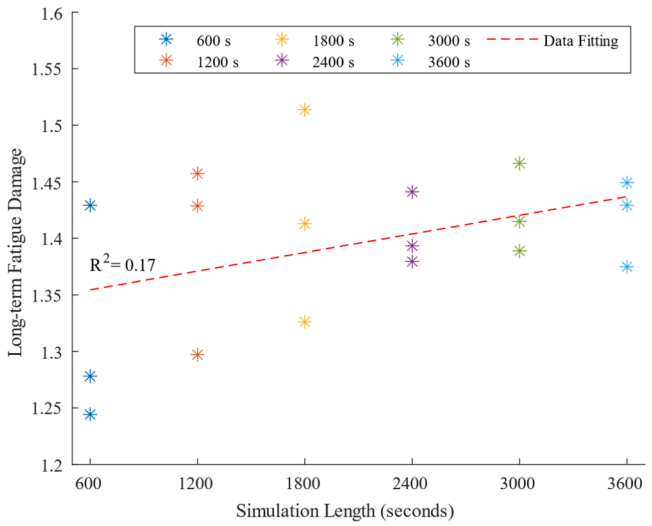

Fig. 15. Relation between the long-term fatigue damage and the simulation length.

Table 4
Stochastic variables considered in the fatigue damage assessment.

Parameter	Distribution	Mean Value	Standard Deviation
D	Lognormal	1	0.30
$\log\tilde{a}_1$	Normal	12.5644	0.20
$\log\tilde{a}_2$	Normal	16.006	0.20
X_{GLA}	Lognormal	1	0.10
X_{SCF}	Lognormal	1	0.20
X_{SS}	Lognormal	1.04	0.02

propagate over time.

The probabilistic fatigue damage assessment using crude MCS results in the probability of fatigue failure for a given period of time, which is referred to as fatigue reliability analysis. Fig. 18 shows the results of the fatigue reliability analysis, and the results indicate that the welded tubular in question does not have sufficient capacity to fulfil its intended purpose until the end of service life under the given environmental and operational loadings. In light of these results, the structural design must be modified because the consequence of potential fatigue failure might be catastrophic. Alternatively, the epistemic uncertainties can be reduced by acquiring more information regarding the environmental loads or using high-fidelity models for stress concentration factors and global stress calculation.

Fig. 18 also presents a comparison between the time-domain fatigue reliability analysis methodology and the conventional one which defines the limit state function analytically and uses the expected value of the long-term hotspot stress range distribution obtained for using AHSE simulations with 1 random seed and with 3 random seeds as well as shorter AHSE simulations with 10 random seeds. Fig. 18 indicates that the conventional methodology overestimates the structural reliability compared to the MCS using the time histories, which is much closer to the exact solution.

Furthermore, a sensitivity analysis is performed to determine the importance of the contribution of each stochastic variable to the limit state function's total uncertainty i.e., probability of failure. In this regard, one can investigate the direction cosines $\alpha_i = -\frac{1}{\sqrt{\sum_{i=1}^{\infty}\left(\frac{\partial g(x)}{\partial x_i}\right)^2}}\frac{\partial g(x)}{\partial x_i}$ of each stochastic variable x_i, constituting the limit state vector $g(\mathbf{X}) = (x_1, x_2, \ldots, x_n)$ for the limit states described analytically and the structural reliability is calculated using approximate mathematical techniques such as FORM. Alternatively, the sensitivity of the stochastic variables can be formulated for numerical MSC, using variance-based sensitivity methods, such as the first-order Sobol Indices, which measure the contribution of each input alone to the output variance performed. For limit state vector $g(\mathbf{X})$, the Sobol Indices are expressed as [81]:

$$s_i = \frac{\mathrm{Var}(\mathrm{E}[g(\mathbf{X}|x_i) < 0])}{\mathrm{Var}(g(\mathbf{X}) < 0)} \tag{15}$$

where s_i is the Sobol index for stochastic variable i, and Var() is the variance. $\mathrm{E}[g(\mathrm{X}|\mathrm{x_i}) < 0]$ is the conditional expectation of probability of failure vector with respect to the stochastic variable x_i and $\mathrm{Var}(g(\mathrm{X}) < 0)$ denotes the variance of overall probability of failure P_f vector including all stochastic variables. The simulation is performed to achieve a minimum of 30 data points in the P_f vector, and for presentation purposes, Sobol Indeces normalised the total sum of the vector can be presented as:

$$S_i = \frac{s_i^2}{\sum_{i=1}^{all} s_i^2} \tag{16}$$

Fig. 19 shows that normalised Sobol indices S_i calculated for the stochastic variables with respect to the probability of failure at the 25th year i.e., end of service life. The stress concentration factor S_{SCF} accounts for the overall variability the most, followed by the stochastic variable associated with the failure damage at failure S_D based on the Palmgren-Miner summation rule and global load and stress analysis S_{GLA}. This result is quite reasonable given the fact that the coefficient of variation is relatively high, and the S-N curve exponent m exacerbates the impact of the uncertainty coming from the stochastic variables related to hotspot stress range calculations.

6. Damage-tolerant design (DTD) approach

Damage-tolerant design (DTD) is a fracture mechanics-based approach dealing with the fundamental nature of fatigue cracking under cyclic load, and it is applicable not only for design purposes but also for inspection and maintenance planning. The DTD approach offers a better progressive damage modelling accounting for the effects such as load sequence, retardation effects, corrosion, and material properties characterisation.

For the reason given above, this section extends the scope of the present study beyond the conservative design-oriented S-N approach by performing a probabilistic structural integrity assessment based on the DTD approach. In doing so, a unique example of an alternative DTD approach to the fatigue reliability methodology based on the S-N approach is presented for the design and structural integrity management of FOWT substructures. To this end, the hotspot stress-time histories calculated in the previous sections are incorporated into crack growth analysis based on the analytical fracture mechanics accounting for load sequence and overload-induced retardation.

Linear elastic fracture mechanics (LEFM) is a well-established and widely used approach to analyse crack growth and estimate the remaining fatigue cracking life of structural details with an initial crack. LEFM assumes that the crack tip conditions can be related to a parameter called the stress intensity factor (SIF) range (ΔK). This relationship can investigate the crack growth under three regions separated by threshold SIF range ΔK_{th} and critical SIF K_c: a) crack initiation, b) stable crack growth, and c) fast fracture. The Paris Law [82] formulates the stable growth region by employing SIF with a material strength-related coefficient and exponent. The Paris Law offers a simple but effective way to assess crack growth so long as the crack growth data follows a linear relationship on a logarithmic scale. The Paris law is expressed as follows [83]:

$$a_c = a_0 + \sum_{i=1}^{Nt} f(\Delta K, C, m, R, ..) = a_0 + \sum_{i=1}^{Nt} \Delta a_i \tag{17}$$

where

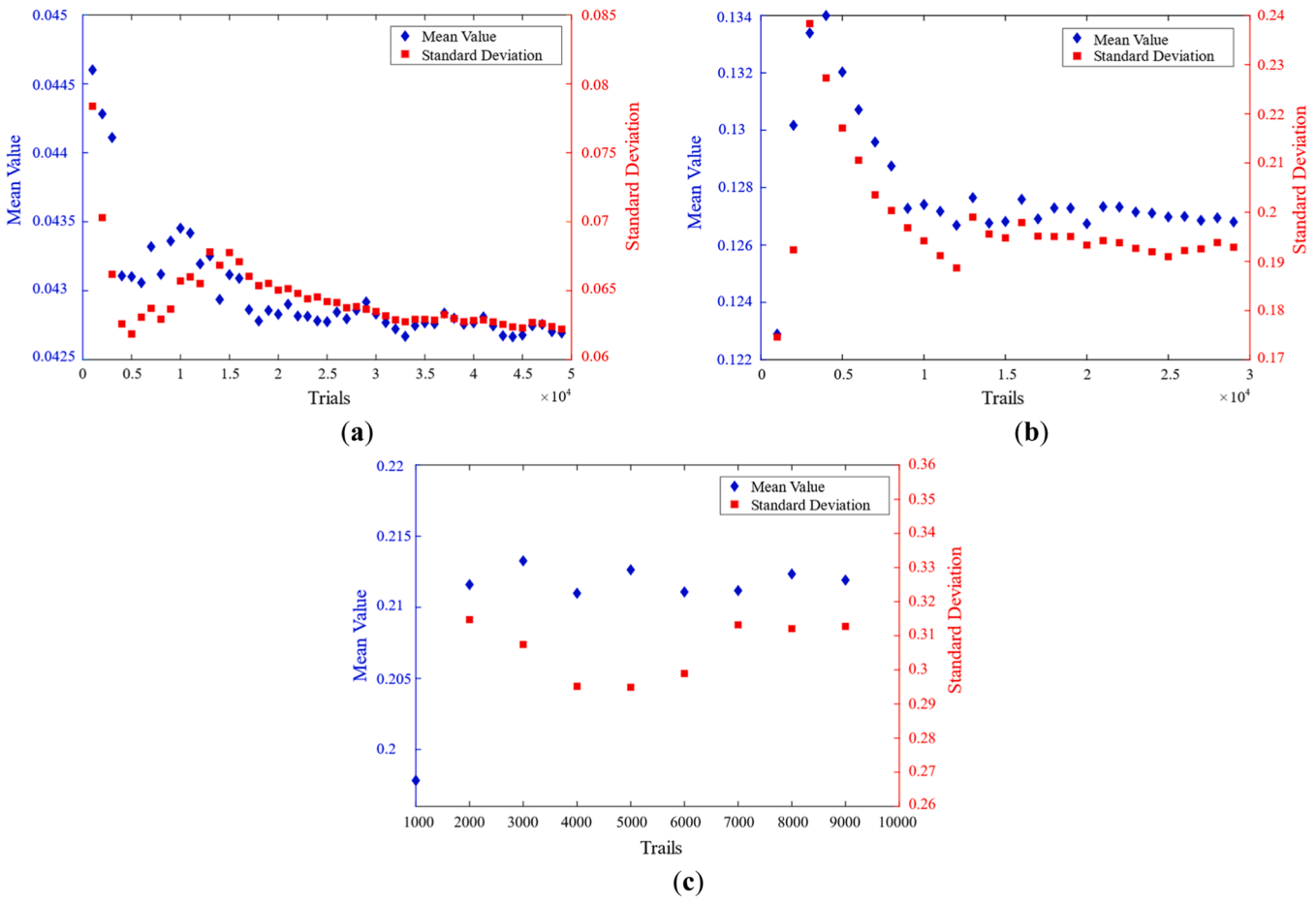

Fig. 16. Monte Carlo Simulation results for long-term FD after (a) 5 years, (b) 15 years, (c) 25 years.

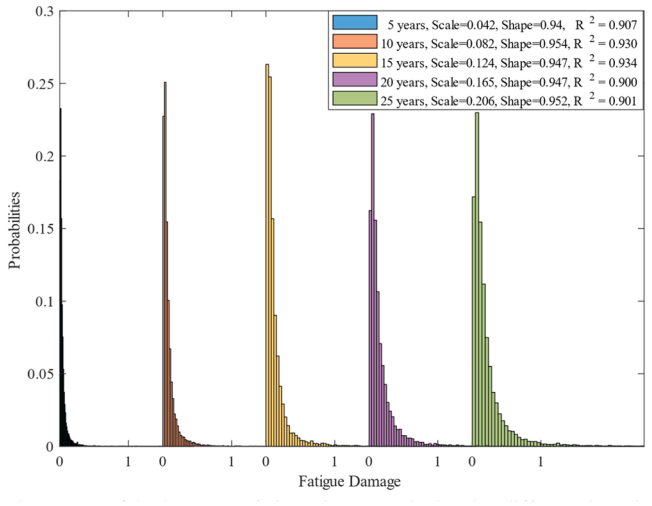

Fig. 17. Histograms of the long-term fatigue damage calculated at different times in service life.

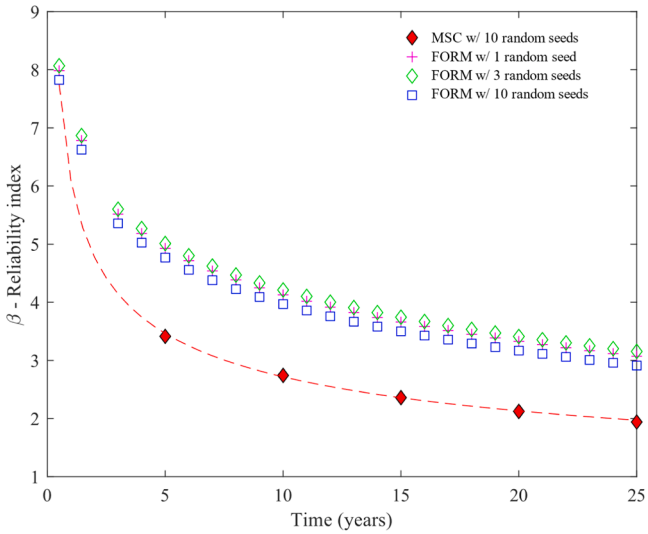

Fig. 18. Fatigue reliability based on the S-N approach throughout the service life of 25 years.

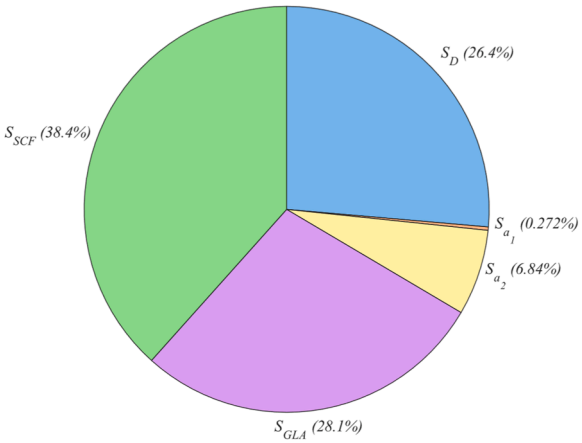

Fig. 19. Results of the sensitivity analysis.

$$\Delta a_i = C_p A(\Delta K_{\text{eff},i})^m \tag{18}$$

$$\Delta K_{\text{eff},i} = Y\Delta\sigma_{\text{HSS}}\sqrt{\pi a_i} \tag{19}$$

$$\Delta K_{\text{eff},i} = \Delta K_i - \Delta K_{th} \tag{20}$$

Further, the Wheeler retardation model introduces a retardation factor, C_p, which is a function of the relative crack growth along the overload-induced plastic zone. This model can be integrated with the Paris law. Thus, the modified Paris law based on the Wheeler yield zone model can be expressed as [84]:

$$C_p = \begin{cases} \left[\dfrac{r_{pi}}{a_{OL} + r_{pOL} - a_i}\right]^{\mu}, & a_i + r_{pi} < a_{OL} + r_{pOL} \\ 1, & a_i + r_{pi} \geq a_{OL} + r_{pOL} \end{cases} \tag{21}$$

where C_p varies from 0 to 1, depending on the location of the crack tip in a previously created larger zone. where a_i represents the current crack length corresponding to the i^{th} cycle, r_{pi} denotes the current plastic zone size, corresponding to the i^{th} cycle, a_{OL} is the crack length at which overload was applied, K_{OL} is the stress intensity factor at which overload was applied, K_{max} is the maximum stress intensity factor following an overload, r_{pi} is the plastic zone created by overload, and β is 1 and 3 for plane stress and plane strain conditions, respectively, and μ is the Wheeler exponent obtained empirically based on the test loading data [85].

$$r_{pOL} = \frac{1}{\beta\pi}\left(\frac{K_{OL}}{\sigma_y}\right)^2 \tag{22}$$

$$r_{pi} = \frac{1}{\beta\pi}\left(\frac{K_{\max}}{\sigma_y}\right)^2 \tag{23}$$

$$a(t) = \begin{cases} \left[a_0^{1-\frac{m}{2}} + \left(1-\frac{m}{2}\right)C\Delta\sigma_{\text{HSS}}{}^m Y^m \pi^{\frac{m}{2}} \nu_0 t\right]^{\frac{1}{\left(1-\frac{m}{2}\right)}}, & \text{for} m \neq 2 \\ a_0 \exp\left(C\Delta\sigma_{\text{HSS}}{}^2 Y^2 \pi \nu_0 t\right), & \text{for} m = 2 \end{cases} \tag{24}$$

where C and m are material constants, and the stress intensity factor is described based on the geometric function Y, the stress range $\Delta\sigma$, and the current crack size ai, which becomes ac after enough cycles N_t to cause fast fracture failure. The geometric function used for a tubular joint must account for the complex stress field occurring due to boundary effects such as loading, non-uniform stress field, and specimen and crack geometries, which can be derived using experimental and finite element analyses [16,86,87].

The through-thickness is defined as the failure criterion for which the probability of failure is calculated because the seawater penetration to the tower has severe consequences. The stochastic variables involved in the probabilistic crack growth assessment are presented in Table 5, and they are related to the Paris Law coefficient A, initial crack size a_0, aspect ratio a_0/c_0, fatigue crack growth X_{FCG}, stress intensity factor X_{SIF}, stress concentration factor X_{SCF}, global load and stress analysis X_{GLA} [16,79,88].

Similar to the fatigue reliability analysis performed based on the S-N approach, the crude MSC is performed to estimate the probability of failure after 5, 10, 15, 20, and 25 years in order to demonstrate how the structural reliability changes over time on the DTD approach. It is worth noting that the failure is defined as the through-thickness.

Fig. 20 shows how the structural reliability reduces over time to the extent that the structure can be considered unsafe. Although the results obtained based on the DTD approach are less conservative compared to the S-N approach, the reliability index goes below the acceptable safety levels before the end of the service life of 25 years. To complement the design modifications, an inspection plan can be devised around the time structural safety is compromised to perform a visual or non-destructive test to detect cracks around the welded tubular joint in question. These tests can reveal the existence of a crack and its size with a certain confidence level; thus, a more comprehensive structural integrity assessment accounting for the load sequence and overload-induced retardation effects can be conducted to have more accurate information on crack propagation and remaining life of the FOWT substructure, as also illustrated in Fig. 20 for a crack propagation of a detected crack depth of 15 mm over a year (~4 $\times 10^6$ cycles).

This is precisely the advantage of using a damage-tolerant design approach for floating offshore wind turbine substructures. Whilst the probabilistic structural integrity assessment can inform both design and inspection planning, a more comprehensive fatigue crack growth assessment can guide operators in finding optimal maintenance and repair activities not only for an asset but also for the whole offshore wind farm. Moreover, if found more cost-efficient, the operators can actively control the wind turbine operation to reduce the fatigue loading so that the remaining life can be prolonged, which allows for an extensive maintenance and repair campaign dealing with multiple floating offshore wind turbines simultaneously. Such a capability entails lower operating leverage and de-risk the offshore wind farm project.

It is important to note that variability in the crack growth can be exacerbated when the overload-induced plasticity is also accounted for. As shown in Fig. 20, the difference in the crack depth at a given time between FCG with (red line) and without the effect of overload-induced plasticity (blue lines) is quite significant. Furthermore, it can be argued that more substantial differences should be expected for the later stages of service life. In addition, the estimated crack growth ranges from approximately 21 mm to 38 mm after a year of service loading, which infers that the FCG considering load sequence and retardation effects, is subjected to a higher degree of uncertainty, which operators need to consider within the scope of a reliability or risk-based inspection and maintenance planning.

Table 5
Stochastic variables considered in the crack growth assessment.

Parameter	Distribution	Mean Value	CoV (%)
a_0	Lognormal	0.15	0.66
a_0/c_0	Lognormal	0.62	0.40
X_{Paris}	Lognormal	1	0.20
X_{FCG}	Lognormal	1.04	0.30
X_{SIF}	Lognormal	1	0.20
X_{SCF}	Lognormal	1	0.20
X_{GLA}	Lognormal	1	0.10

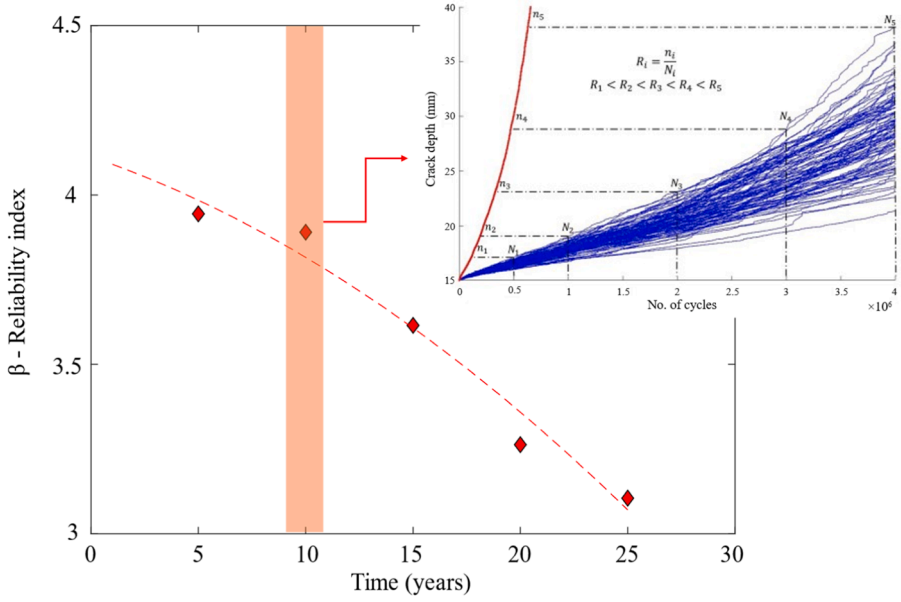

Fig. 20. Fatigue reliability changes over time based on damage-tolerant approach.

7. Conclusions

The present study developed a computationally efficient yet robust reliability-based fatigue analysis and design methodology for FOWT substructures using fully coupled nonlinear AHSE simulations in the time domain. The developed methodology involved multiple phases, such as selecting the sea states contributing the accumulated fatigue damage the most, performing fully coupled AHSE simulations using OpenFAST, calculating the hotspot stress history, estimating the short- and long-term fatigue damage, and finally, carrying out a probabilistic fatigue damage assessment, i.e. fatigue reliability analysis. The structural reliability analysis considered both the S-N and damage-tolerant approaches for fatigue design, accounting for the aleatory and epistemic uncertainties. In light of the analyses presented above, the present study concludes that:

1. Approximately one-eighth fraction of the full scatter (102 sea states) contributes the majority (80 %) of the long-term fatigue damage. In addition, the difference between the simulation length of 600 and 3600 s is not statistically significant. Therefore, by using the algorithm presented in the present study, it is possible to significantly reduce the computational effort needed to obtain the dynamic responses in the time domain, which allows for a higher number of random realisation of these simulations to be integrated into the fatigue reliability analysis using MCS.
2. Higher contributions to long-term fatigue damage were found in the sea states related to the wind speed bin 12-18 m/s. This is due to the fact that wind-induced loading is a predominant source of fatigue load for the majority of the sea states. Also, wave-induced loading becomes quite effective after a wind speed of 20 m/s as the probability of occurrence of these sea states makes the contribution almost negligible, though.
3. The fatigue reliability analysis based on the S-N approach indicated that the analysed welded-tubular joint of the FOWT does not have sufficient structural reliability until the end of FOWT's service life; thus, the structural design must be modified or higher-fidelity models for stress concentration factors and global stress calculation, which might hinder the design optimisation process.
4. The fatigue reliability analysis based on the DTD approach resulted in less conservative results compared to the S-N approach; nonetheless, the reliability index goes below the acceptable safety levels before the end of the service life of 25 years. To address this issue, an inspection plan can be developed in the design phase to perform visual or non-destructive tests to detect cracks around the welded tubular joint in question. Furthermore, depending on the inspection results, the fatigue reliability analysis can be complemented with a more comprehensive structural integrity assessment accounting for the load sequence and overload-induced retardation using the most up-to-date load history of the FOWT.
5. Unlike the S-N approach, the damage-tolerant approach allows for operational flexibility, meaning that the operator can decide when and how to inspect critical structural details and carry out necessary activities depending on the operational and economic circumstances. This flexibility is particularly important for FOWT structures because the main contributor to the fatigue damage is the wind-induced loading resulting from the wind turbine's operation, and implementing active fatigue load control can extend the remaining life before the maintenance and repair activities.

The outcomes of this study help pave the way for a damage-tolerant approach within a multidisciplinary design optimisation of floating offshore wind substructures, resulting in more affordable and safer offshore renewable energy. The methodology developed in this study must be enhanced by including multiple fatigue-critical structural details of the substructure to develop a risk-based design and operation management framework.

CRediT authorship contribution statement

Fengshen Zhu: Writing – original draft, Visualization, Investigation, Formal analysis, Data curation. **Feargal Brennan:** Writing – review & editing, Supervision, Methodology, Funding acquisition, Conceptualization. **Maurizio Collu:** Writing – review & editing, Validation, Supervision, Methodology. **Baran Yeter:** Writing – original draft, Visualization, Validation, Methodology, Investigation, Formal analysis.

Declaration of Competing Interest

The authors declare that they have no known competing financial interests or personal relationships that could have appeared to influence the work reported in this paper.

Data availability

Data will be made available on request.

Acknowledgements

This work was funded by the UK Engineering and Physical Sciences Research Council (EPSRC) as part of the Ocean-REFuel (Ocean Renewable Energy Fuels) Programme Grant EP/W005212/1 (http://www.oceanrefuel.ac.uk/) awarded to the University of Strathclyde, Newcastle University, the University of Nottingham, Cardiff University and Imperial College London. Further, the ARCHIE-WeSt High-Performance Computer (www.archie-west.ac.uk) based at the University of Strathclyde was used to produce the results of the probabilistic structural integrity analysis.

References

[1] Rodriguez CA, Yeter B, Li S, Brennan F, Collu M. A critical review of challenges and opportunities for the design and operation of offshore structures supporting renewable hydrogen production, storage, and transport. Wind Energ Sci Discuss 2024;9:533–54. https://doi.org/10.5194/wes-9-533-2024.
[2] Niblett D, Delpisheh M, Ramakrishnan S, Mamlouk M. Review of next generation hydrogen production from offshore wind using water electrolysis. J Power Sources 2024;592:233904. https://doi.org/10.1016/j.jpowsour.2023.233904.
[3] D.N.V.. RP-C203: Fatigue design of offshore steel structures. Recommended practice 2014,
[4] ABS. Fatigue assessment of offshore structures. American Bureau of Shipping; 2013,
[5] IEC. IEC 61400-3. Wind Turbines—Part 3: Design requirements for offshore wind turbines. Geneva,Switzerland: International Electrotechnical Commission; 2018.
[6] Besten. Hd. Fatigue damage criteria classification, modelling developments and trends for welded joints in marine structures. Ships Offshore Struct 2018;13:787–808. https://doi.org/10.1080/17445302.2018.1463609.
[7] Moan T. Life cycle structural integrity management of offshore structures. Struct Infrastruct Eng 2018;14:911–27. https://doi.org/10.1080/15732479.2018.1438478.
[8] Adedipe O, Brennan F, Kolios A. Review of corrosion fatigue in offshore structures: present status and challenges in the offshore wind sector. Renew Sustain Energy Rev 2016;61:141–54. https://doi.org/10.1016/j.rser.2016.02.017.
[9] Jacob A, Mehmanparast A. Crack growth direction effects on corrosion-fatigue behaviour of offshore wind turbine steel weldments. Mar Struct 2021;75:102881. https://doi.org/10.1016/j.marstruc.2020.102881.
[10] Brennan FP. A framework for variable amplitude corrosion fatigue materials tests for offshore wind steel support structures. Fatigue Fract Eng Mater Struct 2014;37:717–21. https://doi.org/10.1111/ffe.12184.
[11] Yeter B, Garbatov Y, Guedes Soares C. Assessment of the retardation of in-service cracks in offshore welded structures subjected to variable amplitude load. In: Guedes Soares C, editor. Renewable Energies Offshore. London, UK: Taylor & Francis Group; 2015. p. 855–63.
[12] Igwemezie V, Mehmanparast A, Kolios A. Current trend in offshore wind energy sector and material requirements for fatigue resistance improvement in large wind turbine support structures – a review. Renew Sustain Energy Rev 2019;101:181–96. https://doi.org/10.1016/j.rser.2018.11.002.
[13] Shittu AA, Mehmanparast A, Hart P, Kolios A. Comparative study between SN and fracture mechanics approach on reliability assessment of offshore wind turbine jacket foundations. Reliab Eng Syst Saf 2021;215:107838.
[14] Yeter B, Garbatov Y. Structural integrity assessment of fixed support structures for offshore wind turbines: a review. Ocean Eng 2022;244:110271. https://doi.org/10.1016/j.oceaneng.2021.110271.
[15] Yeter B, Garbatov Y, Guedes Soares C. Risk-based maintenance planning of offshore wind farms. Reliab Eng Syst Saf 2020;202:107062. https://doi.org/10.1016/j.ress.2020.107062.
[16] Yeter B, Garbatov Y, Soares CG. Life-extension classification of offshore wind assets using unsupervised machine learning. Reliab Eng Syst Saf 2022;219:108229. https://doi.org/10.1007/s11804-022-00298-3.
[17] Kvittem MI, Moan T, Gao Z, Luan C. Short-Term Fatigue Analysis of Semi-Submersible Wind Turbine Tower. ASME 2011 30th International Conference on Ocean. Offshore and Arctic Engineering; 2011. p. 751–9. https://doi.org/10.1115/OMAE2011-50092.
[18] Fan T-Y, Lin C-Y, Huang C-C, Chu T-L. Time-domain fatigue analysis of multi-planar tubular joints for a jacket-type substructure of offshore wind turbines. Int J Offshore Polar Eng 2020;30:112–9. https://doi.org/10.17736/ijope.2020.jc762.
[19] Xu K, Zhang M, Shao Y, Gao Z, Moan T. Effect of wave nonlinearity on fatigue damage and extreme responses of a semi-submersible floating wind turbine. Appl Ocean Res 2019;91:101879. https://doi.org/10.1016/j.apor.2019.101879.
[20] Marino E, Giusti A, Manuel L. Offshore wind turbine fatigue loads: the influence of alternative wave modeling for different turbulent and mean winds. Renew Energy 2017;102:157–69. https://doi.org/10.1016/j.renene.2016.10.023.
[21] Patryniak K, Collu M, Coraddu A. Multidisciplinary design analysis and optimisation frameworks for floating offshore wind turbines: State of the art. Ocean Eng 2022;251:111002. https://doi.org/10.1016/j.oceaneng.2022.111002.
[22] Li X, Zhang W. Long-term fatigue damage assessment for a floating offshore wind turbine under realistic environmental conditions. Renew Energy 2020;159:570–84. https://doi.org/10.1016/j.renene.2020.06.043.
[23] Song Y, Chen J, Sørensen JD, Li J. Multi-parameter full probabilistic modeling of long-term joint wind-wave actions using multi-source data and applications to fatigue analysis of floating offshore wind turbines. Ocean Eng 2022;247:110676. https://doi.org/10.1016/j.oceaneng.2022.110676.
[24] Song Y, Sun T, Zhang Z. Fatigue reliability analysis of floating offshore wind turbines considering the uncertainty due to finite sampling of load conditions. Renew Energy 2023;212:570–88. https://doi.org/10.1016/j.renene.2023.05.070.
[25] Song Y, Sørensen JD, Zhang Z, Sun T, Chen J. Load condition determination for efficient fatigue analysis of floating offshore wind turbines using a GF-discrepancy-based point selection method. Ocean Eng 2023;276:114211. https://doi.org/10.1016/j.oceaneng.2023.114211.
[26] Hegseth JM, Bachynski EE, Leira BJ. Effect of environmental modelling and inspection strategy on the optimal design of floating wind turbines. Reliab Eng Syst Saf 2021;214:107706. https://doi.org/10.1016/j.ress.2021.107706.
[27] Wiley W, Jonkman J, Robertson A, Shaler K. Sensitivity analysis of numerical modeling input parameters on floating offshore wind turbine loads. Wind Energ Sci 2023;8:1575–95. https://doi.org/10.5194/wes-8-1575-2023.
[28] Zwick D, Muskulus M. The simulation error caused by input loading variability in offshore wind turbine structural analysis. Wind Energy 2015;18:1421–32. https://doi.org/10.1002/we.1767.
[29] Okpokparoro S, Sriramula S. Reliability analysis of floating wind turbine dynamic cables under realistic environmental loads. Ocean Eng 2023;278:114594. https://doi.org/10.1016/j.oceaneng.2023.114594.
[30] Ramezani M, Choe D-E, Heydarpour K, Koo B. Uncertainty models for the structural design of floating offshore wind turbines: A review. Renew Sustain Energy Rev 2023;185:113610. https://doi.org/10.1016/j.rser.2023.113610.
[31] Liao D, Zhu S-P, Correia JAFO, De Jesus AMP, Veljkovic M, Berto F. Fatigue reliability of wind turbines: historical perspectives, recent developments and future prospects. Renew Energy 2022;200:724–42. https://doi.org/10.1016/j.renene.2022.09.093.
[32] Müller K, Cheng PW. Application of a Monte Carlo procedure for probabilistic fatigue design of floating offshore wind turbines. Wind Energ Sci 2018;3:149–62. https://doi.org/10.5194/wes-3-149-2018.
[33] Müller K, Dazer M, Cheng PW. Damage assessment of floating offshore wind turbines using response surface modeling. Energy Procedia 2017;137:119–33. https://doi.org/10.1016/j.egypro.2017.10.339.
[34] Saraygord Afshari S, Enayatollahi F, Xu X, Liang X. Machine learning-based methods in structural reliability analysis: a review. Reliab Eng Syst Saf 2022;219:108223. https://doi.org/10.1016/j.ress.2021.108223.
[35] Haid L., Stewart G., Jonkman J., Robertson A., Lackner M., Matha D. Simulation-Length Requirements in the Loads Analysis of Offshore Floating Wind Turbines. 2013.10.1115/OMAE2013–11397.
[36] Yeter B, Brennan F. Probabilistic structural integrity assessment of a floating offshore wind turbine under variable amplitude loading. Procedia Struct Integr 2024;57:133–43. https://doi.org/10.1016/j.prostr.2024.03.016.
[37] Zhao Z, Wang W, Shi W, Li X. Effects of second-order hydrodynamics on an ultra-large semi-submersible floating offshore wind turbine. Structures 2020;28:2260–75. https://doi.org/10.1016/j.istruc.2020.10.058.
[38] Cao Q, Xiao L, Guo X, Liu M. Second-order responses of a conceptual semi-submersible 10 MW wind turbine using full quadratic transfer functions. Renew Energy 2020;153:653–68. https://doi.org/10.1016/j.renene.2020.02.030.
[39] Mei X, Xiong M. Effects of second-order hydrodynamics on the dynamic responses and fatigue damage of a 15 MW floating offshore wind turbine. J Mar Sci Eng 2021. https://doi.org/10.3390/jmse9111232.
[40] Li H, Bachynski-Polić EE. Analysis of difference-frequency wave loads and quadratic transfer functions on a restrained semi-submersible floating wind turbine. Ocean Eng 2021;232:109165. https://doi.org/10.1016/j.oceaneng.2021.109165.
[41] Robertson A, Wang L. OC6 Phase Ib: floating wind component experiment for difference-frequency hydrodynamic load validation. Energies 2021. https://doi.org/10.3390/en14196417.
[42] Doubrawa P, Churchfield MJ, Godvik M, Sirnivas S. Load response of a floating wind turbine to turbulent atmospheric flow. Appl Energy 2019;242:1588–99. https://doi.org/10.1016/j.apenergy.2019.01.165.
[43] Putri RM, Obhrai C, Jakobsen JB. Response sensitivity of a semisubmersible floating offshore wind turbine to different wind spectral models. J Phys: Conf Ser 2020;1618:022012. https://doi.org/10.1088/1742-6596/1618/2/022012.
[44] Xue L, Wang J, Zhao L, Wei Z, Yu M, Xue Y. Wake interactions of two tandem semisubmersible floating offshore wind turbines based on FAST.Farm. J Mar Sci Eng 2022;10. https://doi.org/10.3390/jmse10121962.
[45] Yao T, Lu Q, Wang Y, Zhang Y, Kuang L, Zhang Z, et al. Numerical investigation of wake-induced lifetime fatigue load of two floating wind turbines in tandem with different spacings. Ocean Eng 2023;285:115464. https://doi.org/10.1016/j.oceaneng.2023.115464.
[46] Luan C., Moan T. On Short-Term Fatigue Analysis for Wind Turbine Tower of Two Semi-Submersible Wind Turbines Including Effect of Startup and Shutdown Processes. 2018.https://doi.org/10.1115/IOWTC2018–1078.
[47] Yang Y, Bashir M, Wang J, Michailides C, Loughney S, Armin M, et al. Wind-wave coupling effects on the fatigue damage of tendons for a 10 MW multi-body floating

wind turbine. Ocean Eng 2020;217:107909. https://doi.org/10.1016/j.oceaneng.2020.107909.
[48] Zhou S, Shan B, Xiao Y, Li C, Hu G, Song X, et al. Directionality effects of aligned wind and wave loads on a Y-shape semi-submersible floating wind turbine under rated operational conditions. Energies 2017. https://doi.org/10.3390/en10122097.
[49] Seo B, Shin H. Experimental study of slamming effects on wedge and cylindrical surfaces. Appl Sci 2020;10. https://doi.org/10.3390/app10041503.
[50] Zhao Z, Wang W, Shi W, Qi S, Li X. Effect of floating substructure flexibility of large-volume 10 MW offshore wind turbine semi-submersible platforms on dynamic response. Ocean Eng 2022;259:111934. https://doi.org/10.1016/j.oceaneng.2022.111934.
[51] Silva de Souza CE, Bachynski EE. Effects of hull flexibility on the structural dynamics of a tension leg platform floating wind turbine. J Offshore Mech Arct Eng 2019;142. https://doi.org/10.1115/1.4044725.
[52] Verma M, Nartu MK, Subbulakshmi A. Optimal TMD design for floating offshore wind turbines considering model uncertainties and physical constraints. Ocean Eng 2022;243:110236. https://doi.org/10.1016/j.oceaneng.2021.110236.
[53] Olondriz J, Jugo J, Elorza I, Aron Pujana-Arrese SA. A feedback control loop optimisation methodology for floating offshore wind turbines. Energies 2019;12. https://doi.org/10.3390/en12183490.
[54] Grant E, Johnson K, Damiani R, Phadnis M, Pao L. Buoyancy can ballast control for increased power generation of a floating offshore wind turbine with a light-weight semi-submersible platform. Appl Energy 2023;330:120287. https://doi.org/10.1016/j.apenergy.2022.120287.
[55] Souza CESd, Bachynski-Polić EE. Design, structural modeling, control, and performance of 20 MW spar floating wind turbines. Mar Struct 2022;84:103182. https://doi.org/10.1016/j.marstruc.2022.103182.
[56] Park S, Glade M, Lackner MA. Multi-objective optimization of orthogonal TLCDs for reducing fatigue and extreme loads of a floating offshore wind turbine. Eng Struct 2020;209:110260. https://doi.org/10.1016/j.engstruct.2020.110260.
[57] Otter A, Murphy J, Pakrashi V, Robertson A, Desmond C. A review of modelling techniques for floating offshore wind turbines. Wind Energy 2022;25:831–57. https://doi.org/10.1002/we.2701.
[58] Matha D, Sandner F, Molins C, Campos A, Cheng PW. Efficient preliminary floating offshore wind turbine design and testing methodologies and application to a concrete spar design. Philos Trans R Soc A: Math, Phys Eng Sci 2015;373:20140350. https://doi.org/10.1098/rsta.2014.0350.
[59] Karimirad M, Moan T. Stochastic dynamic response analysis of a tension leg spar-type offshore wind turbine. Wind Energy 2013;16:953–73. https://doi.org/10.1002/we.1537.
[60] Ferri G, Marino E. Site-specific optimizations of a 10 MW floating offshore wind turbine for the Mediterranean Sea. Renew Energy 2023;202:921–41. https://doi.org/10.1016/j.renene.2022.11.116.
[61] Lemmer F, Yu W, Luhmann B, Schlipf D, Cheng PW. Multibody modeling for concept-level floating offshore wind turbine design. Multibody Syst Dyn 2020;49:203–36. https://doi.org/10.1007/s11044-020-09729-x.
[62] Rohrer P, Bachynski-Polić EE, Collette M. Towards gradient-based design optimization of fully-flexible tension-leg platform wind turbines. J Phys: Conf Ser 2022;2362:012033. https://doi.org/10.1088/1742-6596/2362/1/012033.
[63] Balli E, Zheng Y. Pseudo-coupled approach to fatigue assessment for semi-submersible type floating offshore wind turbines. Ocean Eng 2022;261:112119. https://doi.org/10.1016/j.oceaneng.2022.112119.
[64] Wu J., Chen N.-Z. Fracture Mechanics Based Fatigue Assessment for a Spar-Type Floating Wind Turbine. ASME 2017 36th International Conference on Ocean, Offshore and Arctic Engineering, OMAE 2017. Trondheim, Norway 2017.⟨https://doi.org/10.1115/OMAE2017–61568⟩.
[65] Allen C, Viscelli A, Dagher H, Goupee A, Gaertner E, Abbas N, et al. Definition of the UMaine VolturnUS-S reference platform developed for the IEA Wind 15-megawatt offshore reference wind turbine. Golden, CO (United States): National Renewable Energy Lab.(NREL); 2020.
[66] climate.copernicus.eu. ⟨https://cds.climate.copernicus.eu/cdsapp#!/dataset/reanalysis-era5-single-levels?tab=overview⟩.
[67] IEC 61400–3. Wind Turbines. Part 3: Design requirements for offshore wind turbines. Geneva, Switzerland 2009.
[68] Jonkman J. The new modularization framework for the FAST wind turbine CAE tool. 51st AIAA Aerospace Sciences Meeting Including the New Horizons Forum and Aerospace Exposition. Grapevine (Dallas/Ft. Worth Region), TX 2013. p. 202.⟨http://arc.aiaa.org/doi/pdf/10.2514/6.2013–202⟩.
[69] OpenFAST. openFast documentation, version v3.4.1, https://openfast.readthedocs.io/en/main/ accessed:2023–05-05. 2023.
[70] Hobbacher AF. Fatigue Actions (Loading). In: Hobbacher AF, editor. Recommendations for Fatigue Design of Welded Joints and Components. Cham: Springer International Publishing; 2016. p. 11–36. https://doi.org/10.1007/978-3-319-23757-2_2.
[71] Saini DS, Karmakar D, Ray-Chaudhuri S. A review of stress concentration factors in tubular and non-tubular joints for design of offshore installations. J Ocean Eng Sci 2016;1:186–202. https://doi.org/10.1016/j.joes.2016.06.006.
[72] Jimenez-Martinez M. Fatigue of offshore structures: a review of statistical fatigue damage assessment for stochastic loadings. Int J Fatigue 2020;132:105327. https://doi.org/10.1016/j.ijfatigue.2019.105327.
[73] Miner MA. Cumulative damage in fatigue. J Appl Mech -Trans ASME 1945;12:159–64. <Go to ISI>://WOS:A1945UX93100006.
[74] Rychlik I. A new definition of the rainflow cycle counting method. Int J Fatigue 1987;9:119–21.
[75] Thoft-Christensen P, Murotsu Y. Application of structural systems reliability theory. Berlin: Springer; 1986.
[76] Wang L, Kolios A, Liu X, Venetsanos D, Cai R. Reliability of offshore wind turbine support structures: a state-of-the-art review. Renew Sustain Energy Rev 2022;161:112250. https://doi.org/10.1016/j.rser.2022.112250.
[77] Hasofer AM, Lind NC. An exact and invariant first-order reliability format. J Eng Mech Div 1974;100:111–21.
[78] Dong Y, Garbatov Y, Guedes Soares C. Review on uncertainties in fatigue loads and fatigue life of ships and offshore structures. Ocean Eng 2022;264:112514. https://doi.org/10.1016/j.oceaneng.2022.112514.
[79] JCSS. JCSS Probabilistic Model Code, Resistance models: Fatigue models for metallic structures, http://www.jcss.ethz.ch/. 2006.
[80] Negro V, López-Gutiérrez J-S, Esteban MD, Matutano C. Uncertainties in the design of support structures and foundations for offshore wind turbines. Renew Energy 2014;63:125–32. https://doi.org/10.1016/j.renene.2013.08.041.
[81] Papaioannou I, Straub D. Variance-based reliability sensitivity analysis and the FORM α-factors. Reliab Eng Syst Saf 2021;210:107496. https://doi.org/10.1016/j.ress.2021.107496.
[82] Paris P, Erdogan F. A critical analysis of crack propagation laws. J Basic Eng 1963;85:528–34.
[83] Anderson TL. Fracture mechanics: fundamentals and applications. 3rd ed..,. Boca Raton, FL: CRS press, Taylor & Francis Group; 2005.
[84] Wheeler OE. Spectrum loading and crack growth. J Basic Eng 1972;94:181.
[85] Skinn DA, Gallagher JP, Berens AP, Huber PD, Smith J. Damage tolerant design (Data) Handbook. Wright-Patterson Air Force Base, Ohio: Wright Laboratory. Air Force Mater Command 1994.
[86] Etube LS, Brennan FP, Dover WD. A new method for predicting stress intensity factors in cracked welded tubular joints. Int J Fatigue 2000;22:447–56. https://doi.org/10.1016/S0142-1123(00)00024-4.
[87] Etube LS, Brennan FP, Dover WD. Review of empirical and semi-empirical Y factor solutions for cracked welded tubular joints. Mar Struct 1999;12:565–83. https://doi.org/10.1016/S0951-8339(99)00033-7.
[88] Yeter B, Garbatov Y, Guedes Soares C. Reliability of Offshore Wind Turbine Support Structures Subjected to Extreme Wave-Induced Loads and Defects. Proceedings of The 35th International Conference on Ocean, Offshore and Arctic Engineering, OMAE16. Busan, South Korea: American Society of Mechanical Engineers; 2016. p. V003T02A60.